Reply to the comments of Reviewer #1

Thank you for the time and efforts you have spent on reviewing our manuscript; this is truly appreciated. Based on your comments (copied below) we reply with a point-by-point discussion of your concerns (italic and in blue color). We also include a detailed description of how we have considered your suggestions in the revised manuscript version.

Reviewer #1: The re-submitted version of the study entitled "Spectral Optical Layer Properties of Cirrus from Collocated Airborne Measurements and Simulations" is focusing on a different case study and has generally improved. However, readability can still be improved for example by simplifying sentence structures and writing shorter sentences. Also, the authors should pay attention to precise language (when describing parameters) and complete labeling of the figures (see minor comments below).
Reply: *Thank you for reading the manuscript carefully. We revised the manuscript, e.g. by simplifying sentences and including absolute values into Section 5. We are no native speakers but did our best in polishing the text.*

Reviewer #1: The title and the abstract suggest that more than one case study is analyzed. Only later in the text it becomes clear that ONE case study (now: 30 August 2013) is studied in detail here. I suggest you add this information in the title and the abstract which otherwise are misleading (the reader expects results "collected in two field campaigns over the North Sea and the Baltic Sea in spring and late summer 2013.", p. 1, line 9-14).
Reply: *Thank you for this advice, which we have followed by adding an additional illustrating sentence.*

*"*Exemplary results of one measurement flight are discussed to illustrate the benefits of collocated sampling.*"*

Reviewer #1: p.7, line 191: So if I understand correctly, the lower cirrus layer as well as a water cloud is situated below the cirrus layer that is analyzed in detail from now on? – Please clarify and add a sentence on that.
Reply: *Thank you for this hint! We have added an additional sentence.*

"Additionally, a second cirrus layer is located between 6.7 km and 8.5 km altitude and a low – level water cloud between about 1 km and 1.25 km altitude."

Reviewer #1: p.9-10, line 290-294: Not sure what you mean by a "typical cirrus". – Cirrus geometrical thicknesses vary greatly. You might consider to rephrase as "a rather geometrically thin cirrus". …
On line 294 you mention that the lower cirrus with optical thickness of 1 is "a typical" one. – I suggest to delete that or give a range of "typical" cirrus optical thicknesses based on a reference.
Reply: *Thank you for making this point. Now two references giving ranges of cirrus optical thickness are added in the paragraph.*

"The implemented number size distribution (Fig. 9) and the assumption of a mixture of shapes, described by Baum et al. (2005), results in a cirrus optical thickness of 1, representing a typical cirrus cloud, see Sassen et al. (2001) (τ = 0.03 – 1.66) and Platt et al. (1980) (τ = 0.5 – 3.5)."

Reviewer #1: Only here you state that from now on you are focusing on the lower cirrus layer between 6.7-8.5km. – It'd be easier to follow if you introduce the two layers as well as which part of the analysis you will do for them earlier on.
Reply: *Please, see comment (about p. 7, line 191) above.*

Reviewer #1: p.12: It is a good idea to include a figure (Fig.13) describing the influence of a water cloud with different properties on the cirrus radiative forcing. Unfortunately, much of the description of Fig.13 is unclear. Relative or absolute differences are listed (p.12, lines 371-373, e.g., 72% to 83%...10 Wm-2 to 32Wm2 etc) but it is not clear what these differences refer to. – Please clarify the paragraphs describing Fig.13.
Reply: *Thank you for reading this carefully, we extended the paragraph describing Fig. 13.*

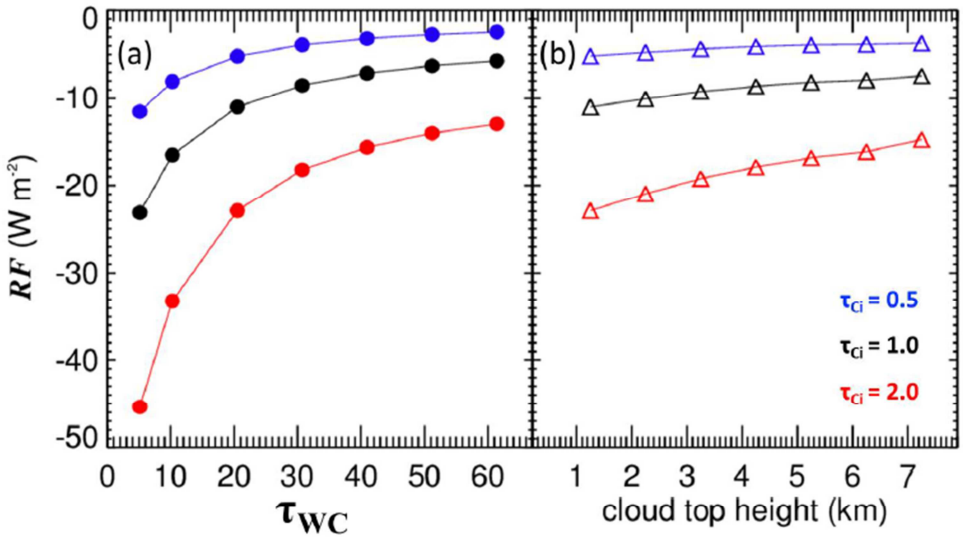

Figure 13. Integrated values of cirrus radiative forcing when a low water cloud is present. The optical thickness (left panel), and the top height (right panel) of the water cloud are varied. The colors indicate the different cirrus optical thicknesses.

"The results obtained in this paper are valid for the respective cloud cases. To evaluate the low–level cloud effect on the cirrus the properties of the low water cloud, such as optical thickness and cloud top height, have to be investigated, too. Therefore, Fig. 13 (a) and (b) show values of integrated cirrus radiative forcings (wavelength range: 300–2300 nm) with varying water cloud optical thickness (a) and cloud top height (b). The cirrus is located between 6.7 km and 8.5 km altitude and consists of the mixture of shapes according to Baum et al. (2005). The color code represents the changing cirrus optical thickness.
In Fig.13 (a) the low–level cloud is located between 1 km and 1.25 km with an increasing optical thickness from 5 to 60. In general, the cooling of the cirrus decreases with increasing optical thickness of the low–level cloud resulting in an increasing influence of the low cloud on the radiative forcing of the upper lying cirrus. An increase of radiation reflected by the lower cloud is available to interact with the cirrus compared to single cloud layer conditions. With increasing water cloud optical thickness a saturating effect becomes evident resulting in a difference of 83% (32 Wm^{-2}) for the cirrus with $\tau = 2$ and a difference of the water cloud optical thickness of 55. Additionally, with increasing cirrus optical thickness the absolute difference of RF_{Ci} increases from 10 Wm^{-2} ($\tau_{Ci} = 0.5$) to 32 Wm^{-2} ($\tau_{Ci} = 2$).
In Fig.13 (b) the low water cloud has a constant optical thickness of 20, and a vertical thickness of 250 m with an increasing cloud top height from 1.25 to 7.25 km in steps of 1 km. Here, the amount of the reflected radiation by the low cloud, available in the cirrus level, depends on the vertical extension of the atmosphere in between and its interaction with the transmitted (from cirrus) and reflected (from water cloud) radiation. Fig.13 (b) shows a decreasing solar cooling with an increasing cloud top height of the low–level cloud. This results in a difference of 8 Wm^{-2} ($\tau_{Ci} = 2$) for a vertical difference of the cloud top height of 6 km. The trend of RF_{Ci} represents a similar saturating effect with increasing cloud top height resulting in percentage differences of 20 % ($\tau_{Ci} = 0.5$) to 35 % ($\tau_{Ci} = 2$).
It is noticeable that the effect due to the optical thickness of the low cloud (a) in comparison to the effect of the cloud top height (b) has a stronger influence on the radiative forcing of the above lying cirrus."

Reviewer #1: p.12-13, lines 396-399: This sentence is unclear. What do the 11% refer to? In general, sometimes it might be better to make two sentences instead of a very long one in which it is difficult to follow what the sub -sentences are referring to…
Reply: *Thank you for the advice.*

"The resulting layer properties at one wavelength in the near infrared range (1640 nm) differ only slightly due to horizontal inhomogeneities and the influence of low--level clouds. An increased effect due to low clouds can be seen in the cloud top albedo with varying values between 0.35 to 0.39, resulting in a percentage difference of up to 11 %.

Reviewer #1: p.1, line 3: not "the" cirrus layer but "a" cirrus layer.
Reply: *We changed the sentence to:*

"Spectral solar optical layer properties of cirrus are derived from simultaneous and vertically collocated measurements of spectral upward and downward solar irradiances above and below a cirrus layer."

Reviewer #1: p.5, line 139-140: The sentence about air mass transport into the stratosphere is totally out of context here. Either delete or expand on it, so it fits into the context.
Reply: *We have deleted the sentence and the reference about the topic of air mass transport into the stratosphere in this paragraph.*

Reviewer #1: p.5, line 145: Introduce that you are analyzing a double-layer cirrus case as shown in Fig.5.
Reply: *The double-layer cirrus case is shown and described in the first paragraph of the following subsection "Microphysical Measurements".*

"Considering the measured ice particle number concentration the cirrus was identified in altitudes between 6.7 km and 8.5 km and between 9.0 km and 9.2 km, with a temperature range of -21°C to -39°C."

Reviewer #1: p.6, line 165-166: This sentence doesn't make sense to me. The optically thicker cirrus which has a geometrical depth of 200m is the upper one (9-9.2 km). Here it sounds like as if you are referring to the lower one between 6.7-8.5 km (geometrical thickness of 1.8 km).
Reply: *We have modified this misleading sentence to:*

"This results in an increasing optical thickness of the upper cirrus layer in comparison to the underlying cirrus layer assuming a comparable vertical extent of 200 m."

Reviewer #1: p.6, line 174: "manoeuver**s**"
Reply: *We removed the typo:*

"The gray colored peaks in the time series of the irradiance (Fig. 6 (a)) are due to flight manoeuvers and have to be excluded from further analysis."

Reviewer #1: p.7, line 201: …due to low clouds AND the cirrus layer at 6.7-8.5 km?
Reply: *During this flight period (between the dashed lines in Fig. 6) the lower cirrus layer was absent. By the help of a video filmed from out the cockpit we checked the cloud situation underneath the aircraft. Only the low-level water cloud was present in the measurement area.*

Reviewer #1: p.11, line 334: Choose a more descriptive title such as "Impact of a underlying low-level cloud on cirrus optical properties"
Reply: *Thank you for this advice. We have decided to change the title of Section 5 to "Sensitivity Studies based on radiative transfer simulations" to better introduce to the following section.*

5. Sensitivity Studies based on radiative transfer simulations

"In this section sensitivity studies of the cirrus optical properties using radiative transfer simulations are presented. In the following the one–dimensional radiative transfer model is introduced. It is applied for individual cirrus layers as well as for atmospheric cases including a cirrus and an underlying low–level cloud. "

5.1 Model introduction

5.2 Individual cirrus layer

5.3 Cirrus and underlying low-level cloud

Reviewer #1: p.11, line 338: "two conditions" instead of "two cirrus cases", since you state that the SAME cirrus at 6.7-8.5 km is analyzed here.
Reply: *We followed your advice:*

"Fig.12 shows two conditions, one with (black line) and one without (red line) a low–level water cloud."

Reviewer #1: p.11, line 340: Explain why you use a water cloud with tau = 20 here.
Reply: *We have used MODIS data taken during the time when the measurement took place to estimate the optical thickness of $\tau = 20$ and the cloud top height of 1.25 km.*

Reviewer #1: p.13, line 407: Suddenly you refer to the "measurement flights" – why plural now? You present one case study.
Reply: *We changed the respective sentence to:*

"A similar effect is due to an additional low-level water cloud, as observed during the measurement flight, with a noticeable difference in the reflectivity of the above lying cirrus of up to a factor of 2 under multi-layer conditions."

Reviewer #1: p.13, line 413: always add "%" after each percentage value throughout the text, even if you list several ones.
Reply: *We made the changes requested:*

"The variation of the low–level cloud properties cloud top height and optical thickness influences the cirrus radiative forcing, too, resulting in differences of 35% and 83 %, respectively."

Reviewer #1: p.13, line 416: "influences", not "influenced"
Reply: *Done.*

"This is partly due to a variety of possible ice crystal shapes and mixtures of shapes, and influenced by a changing albedo during the flight."

Reviewer #1: p. 13., line 416: "ice crystal shapes" instead of "shapes"
Reply: *Done.*

"This is partly due to a variety of possible ice crystal shapes and mixtures of shapes, and influenced by a changing albedo."

Reviewer #1: p.13, line 416: "changing surface albedo during the flight" instead of "changing albedo"
Reply: *Done.*

"This is partly due to a variety of possible ice crystal shapes and mixtures of shapes, and influenced by a changing albedo during the flight."

Reviewer #1: p.13, line 419: "properties" instead of "property"
Reply: *Done.*

"The effect of the low–level water cloud has to be further investigated by varying the properties of the cirrus, such as shape, size, and height of the cloud base and top."

Reviewer #1: p.19, caption of Fig.5: "layers" not "layer"
Reply: *Done.*

"The gray areas indicate the vertical extent of the cirrus layers."

Reviewer #1: p.20, caption of Fig.6: There are two vertical dashed lines. So I assume you meant to write "the period between the two vertical dashed lines" …
Reply: *You are correct, we changed the sentence to:*

"The vertical dashed lines mark the period of the measurement example in Fig. 7."

Reviewer #1: p.20, caption of Fig.7: a) unclear which line is dotted and which one solid. I see two solid lines and one dotted line but the caption only refers to one solid and one dotted line. Maybe mark with arrows in the figure itself. Again, not sure if the mean of the measurement period between the two vertical dashed lines in Fig.6 is meant or if a single measurement example is shown. – Clarify.

Reply: *This is a valid point, the two curves of the upward irradiance above and below the investigated cirrus layer are nearly the same. That is why it looks like only one curve.*

The measurement example is the mean value of the period between the two dashed lines.

"(a) shows averaged spectral downward and upward irradiance F from the aircraft above the cloud layer (solid lines) and AIRTOSS below the cloud layer (dotted lines) at the time period, indicated by the vertical dashed lines in Fig. 6."

Reply to the comments of Reviewer #2

Thank you for the time and efforts you have spent on reviewing our manuscript; this is truly appreciated. Based on your comments (copied below) we reply with a point-by-point discussion of your concerns (italic and in blue color). We also include a detailed description of how we have considered your suggestions in the revised manuscript version.

Reviewer #2: This work presents results of collocated (spatially and temporally) shortwave, spectral cloud radiation (downwelling and upwelling) and concurrent microphysical measurements from instrumentation on an aircraft above a thin, cirrus layer and from a platform (called the AIRTOSS) towed below and behind the aircraft. For the case study presented, the atmospheric layer bounded by the aircraft and the towing platform, which had a vertical distance of ~ 200 m, which also contained the (thin) cloud. Using the combination of radiation measurements from the two platforms observations of spectral (from 300 to 2200 nm) cloud absorptivity, transmissivity, and reflectivity of the layer were provided as well as the cloud top albedo. The measurement results presented are the first for true, collocated sampling of radiation fields above and below a cloud; other studies have applied approaches to perform this sampling with a single aircraft consecutively, or with two aircrafts, but with some temporal lag between. The authors mention how these other, previous, measurement sampling configurations can only be applied to clouds with little static development and that are horizontally homogenous (i.e. no 3-D effect); this discussion, at first, implies that the presented aircraft + AIRTOSS sampling configuration is unaffected by these constraints. It becomes more clear (but could probably be more explicitly stated) that the aircraft + AIRTOSS sampling configuration would still be subject to uncertainties in horizontal radiation flow out/in.

Reply: *As we performed truly collocated airborne measurements to derive cirrus optical layer properties we have a paragraph in the manuscript showing the advantages of this real collocation of measurement platforms. We measure the vertical upward and downward irradiance with no flux contributions from horizontal photon transport. As the Equation (3) for the absorptivity implies, there are no horizontal components of radiative flux divergence, only vertical flux divergences are considered to derive absorptivity. We have emphasized this fact in the manuscript at pages 1 and 5.*

For investigating the horizontal photon transport due to the cirrus layer it would be necessary to perform 3-dimensional simulations or measurements with tilted optical sensors. Both was not performed und therefore not presented in this manuscript.

"Spectral upward and downward solar irradiances from vertically collocated measurements above and below a cirrus layer are used to derive cirrus optical layer properties such as spectral transmissivity, absorptivity, reflectivity, and cloud top albedo. The radiation measurements are supplemented by in–situ cirrus crystal size distribution measurements and radiative transfer simulations based on the microphysical data. The close collocation of the radiative and microphysical measurements, above, beneath and inside the cirrus, is accomplished by using a research aircraft (Learjet 35A) in tandem with the towed sensor platform AIRTOSS (AIRcraft TOwed Sensor Shuttle)."

"Equation 3 implicitly assumes that there are no horizontal components of radiative flux divergence, only vertical flux divergences are considered to derive absorptivity by Eq. 3."

Reviewer #2: I do have a criticism regarding the discussion of radiative forcing presented in this work for these reasons:
a) it is not discussed that the radiative forcing is typically defined as the net of shortwave and longwave, and that the warming by cirrus comes from absorbing the outgoing energy from the earth (i.e. the LW component). Please add to the intro material.
b) while it is mentioned in intro and conclusion that the radiative forcing presented in this study is shortwave radiative forcing ("solar cooling"), I think this should be emphasized once. Perhaps along with Equation 6. In light of concern a), please refine text following equation 6 to reflect that the LW component is additionally necessary to evaluate whether a cloud has a net warming or cooling effect on the underlying atmosphere/surface.
Reply: *Thank you for this hint. We have followed your advice and have added some clarifying sentences in this paragraph.*

"The subscripts "cloud" and "clear sky" indicate measurements or simulations in cloudy conditions and in a clear sky atmosphere. Following Eq. (6) RF_{toa} is the net of solar (shortwave) and terrestrial (longwave) radiation between the atmospheric conditions. A positive RF_{toa} indicates a net warming effect of the cloud by absorbing the outgoing energy from the Earth's surface. A negative RF_{toa} indicates a cooling effect by reflecting the incoming solar radiation. The following investigations are focused on the solar spectrum from 300 nm to 2300 nm."

Reviewer #2: c) the discussion in regards to Figure 12 (page 11; lines 355-357) refers to "noticeable" results where there is a change in sign from cooling to warming at near-infrared wavelengths for a cirrus cloud in the presence of an underlying water cloud. I agree I can see a tiny blip in the spectrum, but it is practically indistinguishable from the zero-change line. While I don't argue that systematic uncertainties are very important, I do think this particular aspect of the results has been overly interpreted.
Reply: *Thank you for the advice, we have reordered the paragraph describing Fig. 12. Concerning the sign changing effect of RF_{Ci}, it is a valid point. The absolute values of the positive radiative forcing in the near infrared wavelength range, reported in this manuscript, are very low. A significant point is the changing of RF to a less cooling effect (80 %) as it is obvious in Fig. 12 (e).*

"RF_{Ci} is shown in Fig. 12 (e) (black line) in contrast to the radiative forcing RF (see Eq. 6) of the same but single--layer cirrus (red line). This leads to an overestimation of the cooling effect of the cirrus with a percentage difference of about 80 % (-0.05 to -0.01 W m^{-2} nm^{-1}) in the visible wavelength range and up to a factor of 2 in the near infrared range caused by the low-level cloud. Furthermore, there is a sign changing effect on RF' with negative values for the visible spectral range and a positive radiative forcing in the near infrared range (-0.002 to 0.002 W m^{-2} nm^{-1})."

Reviewer #2: Page 7, line 224 – I think you are mistaken when you attribute the low reflectivity in Fig 7b to the cirrus cloud and a brighter warm cloud underneath. I think this is just a typo as earlier in the manuscript, the clear difference between a layer property and that of cloud layer plus atmosphere was established.
Reply: *Sorry for this error, which has been removed in the revised manuscript version.*

"The reflectivity in Fig. 7 (b) shows very low values of not more than 0.03. This is due to the optically thin cirrus layer."

Reviewer #2: Page 11, line 342 – In the discussion of the cirrus and underlying low-level cloud, the additional contribution from multiple reflections of radiation from the low-level cloud that are reflected upward and then interact with the cirrus cloud have been attributed as a property of the cirrus layer. I think it would be important to make clear that this is only true according to the measurement-based definition of transmissivity defined in Eq (2). In actuality, the true cirrus "layer" properties would be unaffected by the lower level cloud.
Reply: *Your statement is correct, the Equation (2) for transmissivity is to some extent artificial. However, the radiative transfer in the cirrus layer is affected by the low-level water cloud. The cirrus above receives a larger amount of radiation, due to the reflection by the water cloud, which is available for interaction (e.g., reflection, absorption) resulting in changing cirrus optical layer properties.*

Reviewer #2: Figures 10&11&12: It would seem in Figure 10, that the greatest factor to the differences between the various simulations and the measurements (with diamonds) arises from the contributions by the underlying surface (a water cloud) to the cirrus layer.
Is a claim of the paper that there is a potential for the retrieval of particle shape using measurements of cirrus layer absorption– for limited, idealistic cases? (dark ocean, no underlying clouds before the cirrus or 3-D effects)? The sensitivity to the changing surface properties (Fig 12) would seem to swamp any of the spectral signature change due to particle shape (within the uncertainty of the measurements).
Reply: *As you pointed out correctly, the underlying surface and low–level clouds have a significant effect on the cirrus optical properties. In general, they depend on the spectral shape of the surface reflectivity. These factors, as well as different possible properties of the cirrus, such as ice crystal shape and optical thickness, would lead to a variety of circumstances influencing the cirrus properties. . Therefore, we don't think it is realistic to derive crystal shape from these measurements. We have made a corresponding statement in the text.*

"The application of measured in situ microphysical properties as input of radiative transfer simulations did not accurately reproduce the measured cirrus optical layer properties. This is partly due to a variety of possible ice crystal shapes and mixtures of shapes, which was not measured, and the impact of a changing albedo during the flight. Because the low–level water cloud has a significant influence, more information of the water cloud is needed as well. Further adjustment of the simulations can probably be used to optimize the agreement and derive more information on the particle properties. The effect of the low–level water cloud has to be further investigated by varying the properties of the cirrus, such as shape, size, and height of the cloud base and top."

Reviewer #2: In Figure 11b, do I understand correctly that these results would reflect the inverse relationship between particle size and scattering? So, while Table 1 does not include a value of effective diameter (or effective radius), I assume that the ice models with the largest optical thickness would correlate to smallest effective diameter. Then, were the simulations for Approach II also to be shown for a constant optical thickness, any resulting differences could be attributed to a size effect.
Reply: *Thank you for the hint, we have followed your advice and added the effective radii into Table 1. Concerning your remark, the inverse relationship between particle size and optical thickness can be seen in this table.*

Table 1. Shown are the optical thicknesses at λ=550 nm and effective radii (μ m) for a cirrus between 6.7 k and 8.5 km altitude assuming different ice crystal shapes for Approach I (constant number size distribution) a Approach II (constant ice water content).

	Approach I		Approach II	
	τ	R_{eff}	τ	R_{eff}
Droxtal	1.49	88.5	2.68	76.5
Solid Column	1.50	88.5	3.20	56.1
Column 8 Elements	0.77	88.5	7.45	27.3
Plate	1.15	88.5	4.44	28.7
Plate 10 Elements	0.54	88.5	15.4	11.9
Hollow Bullet Rosette	0.97	88.5	9.52	17.2
Baum	1.00	88.5	5.09	23.8

Reviewer #2: Could you supply the wavelength for which the optical thickness values are applied in the caption to Table 1?
Reply: *Thank you for making this point, the wavelength is added in the caption of Table 1.*

"Shown are the optical thicknesses at λ = 550 nm for a cirrus between 6.7 km and 8.5 km altitude assuming different ice crystal shapes for Approach I (constant number size distribution) and Approach II (constant ice water content)."

Reviewer #2: Page 9, line 275 – 'The ice crystal shape is assumed do (to) be constant."
Reply: *Done.*

"The ice crystal shape is assumed to be constant, further assuming a mixture of particle shapes according to Baum et al. (2005)."

Reviewer #2: Page 7, line 214 – '…according the (to) Eq,'
Reply: *Done.*

"By measuring the spectral and collocated upward and downward irradiances at two altitudes the cloud optical layer properties of the cirrus layer are derived according to Eq. (1) – (3)."

Reply to the comments of Reviewer #3

Thank you for the time and efforts you have spent on reviewing our manuscript; this is truly appreciated. Based on your comments (copied below) we reply with a point-by-point discussion of your concerns (italic and in blue color). We also include a detailed description of how we have considered your suggestions in the revised manuscript version.

Reviewer #3: The authors have done an admirable job in finding a better case study to illustrate the measurement of cloud radiative properties. The results in this version are far better than in the initial version of this manuscript. The spectra of absorptance, reflectance, and transmittance are all in agreement with what is generally expected from theory and previous measurements of cloud spectral irradiance. However, the manuscript still requires revision before it is suitable for publication.
Reply: *Indeed, the case we present in the latest manuscript version resembles much more clearly our expectations from both theory and previous measurements. Thanks to the reviewer who pointed us in this direction.*

Reviewer #3: Line: 13: The authors list crystal shape, effective radius, and optical thickness as cloud particle properties important on the spectral optical layer properties (optical thickness is not a particle property). Throughout the paper the authors attribute the spectral irradiance differences to crystal shape. Of the three listed, shape has the smallest effect on the spectral irradiance. The optical thickness and effective radius are the two main drivers of cirrus cloud layer properties. The authors need to better delineate and quantify the differences in the results due shape and those due to size. It is imperative to list the sizes alongside the shapes to be sure that differences can be ascribed to shape only.
Reply: *We have considered this comment by revising Table 1, which lists, next to the respective cirrus optical thicknesses, also the effective radii. We also have changed several text passages in order to emphasize that in the sensitivity tests we focus on shape effects although it is most certain that effective radius and optical thickness mostly determine the optical layer properties of the cirrus. Thanks for making this point, it was not our intention to overemphasize the shape effects, we rather wanted to highlight that shape effects cannot be ignored/neglected because their impact is indeed significant.*

Table 1. Shown are the optical thicknesses at λ=550 nm and effective radii (μ m) for a cirrus between 6.7 km and 8.5 km altitude assuming different ice crystal shapes for Approach I (constant number size distribution) and Approach II (constant ice water content).

	Approach I		Approach II	
	τ	R_{eff}	τ	R_{eff}
Droxtal	1.49	88.5	2.68	76.5
Solid Column	1.50	88.5	3.20	56.1
Column 8 Elements	0.77	88.5	7.45	27.3
Plate	1.15	88.5	4.44	28.7
Plate 10 Elements	0.54	88.5	15.4	11.9
Hollow Bullet Rosette	0.97	88.5	9.52	17.2
Baum	1.00	88.5	5.09	23.8

Reviewer #3: Line 71: remove the word “applied”
Reply: *Done.*

“The aircraft certified for the operation of AIRTOSS is a Learjet 35A.”

Reviewer #3: Line 105: change “quiet flying” to “stable flight”
Reply: *Done.*

“The housing of the towed platform consists of an aerodynamic canister to avoid irregular movements and to enable quiet flying, which is crucial for reliable radiation measurements (Frey et al., 2009).”

Reviewer #3: Line 125-132: Here begins the discussion and definition of the radiative forcing (RF). It would be helpful, to explicitly state that the RF in this paper only addresses the shortwave spectrum. The terrestrial spectrum, critical to radiative forcing involving cirrus clouds, is not addressed in this paper (this is discussed only at the end of the paper).
Reply: *Thank you for this hint, which has also given by another reviewer. We have followed your advice and have added some clarifying sentences in this paragraph.*

“The subscripts "cloud" and "clear sky" indicate measurements or simulations in cloudy conditions and in a clear sky atmosphere. Following Eq. (6) RF_{toa} is the net of solar (shortwave) and terrestrial (longwave) radiation between the atmospheric conditions. A positive RF_{toa} indicates a net warming effect of the cloud by absorbing the outgoing energy from the Earth's surface. A negative RF_{toa} indicates a cooling effect by reflecting the incoming solar radiation. The following investigations are focused on the solar spectrum from 300 nm to 2300 nm.”

Reviewer #3: Line: 137: Reword "The measurement areas represent boxes…" Perhaps "the measurement areas were rectangular with areas of 50x80…"
Reply: *Done.*

"The measurement areas represent rectangles with the size of 50 x 80 km^2, and 35 x 80 km^2, respectively."

Reviewer #3: Line 139: I am not sure why the authors talk about the transport of tropospheric air into the stratosphere here. It either needs to be followed up with more text as to the importance/relevance of this transport to the work described in this paper or removed. Currently it only distracts the reader.
Reply: *Thank you for the advice. We deleted the sentence about the topic of air mass transport into the stratosphere here. It does not add to the topic of this paragraph.*

Reviewer #3: Line 160-165 The microphysical measurements of the cloud layers are given in mean diameter. There needs to be some description of how these were then related to the radiatively important effective radius. Clearly from Figure 11 the method incorporating the microphysical measurements into the radiative transfer calculations (Approach I and II) has a profound effect and thus needs to be described in detail.
Reply: *The mean diameter given in Fig. 5 is derived from the microphysical measurements with the CIPgs on AIRTOSS.*
As input for the simulations the measured number size distributions are used. The effective radius results from the relation between the third (volume) and the second (area) moment of the distribution. This has been clarified in the text.

Reviewer #3: Line 181: Change "dragged" to "towed". Dragged implies something uncontrolled.
Reply: *Done.*

"As the AIRTOSS is towed behind the aircraft time allocation of the radiation measurements of the towed platform has to be adjusted to that measured simultaneously on the Learjet 35A to guarantee clear vertical collocation of the measurements."

Reviewer #3: Line 204: Change "no water vapor absorption…" to "little water vapor absorption." There is undoubtedly water vapor absorption across this layer. The 1400 and 1900 nm band are highly sensitive to very small amounts of water vapor, and water vapor has been measured much higher (and dryer) in the atmosphere utilizing these bands. Remove or change the line about all of the solar radiation absorption is due to cirrus cloud. This is not the case. In fact, the water vapor absorption is visible in the 940, 1400, and 1900 nm water vapor bands in Figure 10.
Reply: *Thank you for making this point. We have corrected the respective text passage in the revised manuscript.*

"Due to the high altitude, about 9.2 km, little water vapor absorption bands are revealed in the near infrared spectra as shown by the almost unaffected downward irradiance in

both levels. Therefore, most of the absorption of solar radiation, measured in the downward irradiance below the cirrus, originates from the cirrus itself."

Reviewer #3: Lines 208-211: I have trouble understanding this section. Yes, low-level, optically thick, clouds have a large effect (dominate the signal) in the upwelling irradiance. Because they are low level the water vapor absorption across the entire spectrum is present. The author talks about liquid water absorption, which no doubt occurs, but is difficult to separate from the overlapping water vapor absorption. This section needs to be corrected.
Reply: *Thank you for your advice, we have considered this point in the paragraph.*

"The upward radiation depends on the albedo of the Earth's surface and underlying clouds, as can be seen in enhanced values of upward irradiance. The absorption bands of liquid water, as well as water vapor absorption, at wavelengths of 1140 nm or 1400 nm are obvious in the spectra. Furthermore, the irradiances $F^{\uparrow}$ at both altitudes are similar. In comparison to the bright surface the difference due to the cirrus is not significant."

Reviewer #3: Line 222: Change "and almost 100%" to "nearly 100%"
Reply: *Done.*

"As cirrus clouds are optically thin, the transmissivity dominates over the entire spectral range with high values between 88 % and nearly 100 %."

Reviewer #3: Line 222: "The reflectivity in Fig 7 (b) shows very low values of not more than 3%. This is due to the optically and vertically thin cirrus layer" Remove "vertically" here, the vertical extent does not affect the reflectivity.
Reply: *As the cirrus optical thickness depends on the ice water content, effective radius, and vertical extent of the cirrus, the reflectivity depends on the optical and geometrical properties as well.*

Reviewer #3: Line 241: "but still within the error bars" What is meant here?
Reply: *The error bars in the left panel of Fig. 8 (a-d) show the possible values of the measured layer properties. The right panel (e-h) represents the respective measurement distributions that differ no more from the mean value than the error bars. We have made that more clear by changing the respective text to:*

"Absorptivity and reflectivity range between 0.078 and 0.098, and 0.001 – 0.008, resulting in a percentage difference of 21 % and 87 %, respectively. This is still within the error bars as shown in the left panels (b) and (c) of Fig. 8."

Reviewer #3: Line 256: Change "needed" to "required".
Reply: *Done.*

"The required volumetric extinction coefficient ‹$b_{ext,\lambda}$›, single–scattering albedo ‹ω_λ›, and phase function ‹p_λ› are derived by combining calculated tables of single scattering properties by Yang et al. (2005) with a specific in situ measured number size distribution dN / dD (in cm^{-3}) from the CCP installed on AIRTOSS."

Reviewer #3: Line 275: "The ice crystal shape is assumed "do" ["to" - typo] be constant, further assuming a mixture of particle shapes according to Baum et al., (2005)". This seems non sensical, the shape is constant but a mixture of shapes? This should be reworded.
Reply: *We changed the text accordingly to:*

"The composition of ice crystal shapes is assumed to be constant, further assuming a mixture of particle shapes according to Baum et al. (2005)."

Reviewer #3: Line 280: Throughout the paper the absolute differences are often left out of the discussion (e.g. a factor of 5 or 10%). Because the values are most often small numbers, the ratios of two small numbers produces large percentage changes but are in fact very small in an absolute sense. This can be misleading to the reader. So please insert the absolute values *everywhere* ratio/percentage differences are given.
Reply: *Thank you for this valuable advice. We have added the absolute values for the percentage differences, given in this manuscript, in Section 5 at the pages 10 – 14.*

Reviewer #3: Line 286: The author attributes the differences between the measurements and the modeling only to the input parameters in the modeling. It is clear that there are measurement/sampling errors. In fact, the discussion of horizontal flux divergence, one of the main obstacles to making these kinds of measurements, has disappeared from the manuscript.
Reply: *As we performed collocated airborne measurements to derive cirrus optical layer properties we have a paragraph in the manuscript showing the advantages of this collocation of measurement platforms. We measure the vertical upward and downward irradiance with no flux contributions from horizontal photon transport. As the Equation (3) for the absorptivity implies, there are no horizontal components of radiative flux divergence, only vertical flux divergences are considered to derive absorptivity.*
For investigating the horizontal photon transport due to the cirrus layer it would be necessary to perform 3-dimensional simulations or measurements with tilted optical sensors. Both was not performed und therefore not presented in this manuscript.

"Spectral upward and downward solar irradiances from vertically collocated measurements above and below a cirrus layer are used to derive cirrus optical layer properties such as spectral transmissivity, absorptivity, reflectivity, and cloud top albedo. The radiation measurements are supplemented by in–situ cirrus crystal size distribution measurements and radiative transfer simulations based on the microphysical data. The close collocation of the radiative and microphysical measurements, above, beneath and inside the cirrus, is accomplished by using a

research aircraft (Learjet 35A) in tandem with the towed sensor platform AIRTOSS (AIRcraft TOwed Sensor Shuttle)."

"Equation 3 implicitly assumes that there are no horizontal components of radiative flux divergence, only vertical flux divergences are considered to derive absorptivity by Eq. 3."

Reviewer #3: The authors previously cited horizontal photon transport as a motivation for the work. No change in the input parameters will produce 3-4% absorption (Figure 10c) in the visible from ice particles no matter the shape, size, or optical thickness. Horizontal photon divergence will. As the modeling demonstrates, absorption from ice only occurs in the near-infrared. Additionally, the errors bars for the measurements must be included in this figure (which are, no doubt, greater than 3-4%).
Reply: *This is a valid point. But unfortunately, for showing the error bars of the measurement case in this figure it would be necessary to expand the axis. This would lead to a worse recognition of the simulated curves. Instead, as it is the same measurement case, the reader is referred to have a look at Fig. 7 (b) to see the error bars of T, R, A, and* R_{top}.

Reviewer #3: Line 302-304: Please expand on the differences between the two approaches. Why is IWC the more physical approach?
Reply: *It makes sense, that if the crystal shape varies in the cirrus for any reason, then it is rather realistic that the IWC does not change during this transition. In this case the number concentration N would have to change with crystal shape. In fact, extinction and absorption in ice clouds depend on the mass and the total projected cross-sectional area of the crystals but not on N (e.g., Mitchell et al., 1996). Thus, from the modeling point of view it is more reasonable to keep the IWC constant, see also Wendisch et al. (2007). We have tried to make this more clearly in the following two sentences of the revised paper version.*

"Two approaches are investigated: (I) the number size distribution is constant (NSD, left panels), (II) the ice water content is constant (IWC, right panels). While the number size distribution is derived from in situ measurements, assuming a constant IWC for a cirrus layer under constant atmospheric conditions is a more physical approach."

Reviewer #3: Why do the two approaches produce such large differences in optical thickness (Table 1.)
Reply: *Approach I is under the assumption of a constant number concentration, while in approach II the IWC is constant. The reference IWC was calculated by using the measured number size distribution and assuming spherical cloud particles.*
Depending on the relation between the projected area and the volume of the respective cloud particle for the different ice crystal shapes the resulting optical thickness varies.

Reviewer #3: Line 310: Following an earlier comment, is this purely a shape change?
Reply: *Thank you for making this point. As it can be seen in the optical thicknesses compiled in Table 1, the increasing radiative forcings for the respective ice crystal shapes follow the same order of increasing optical thickness. Assuming a constant number size distribution for varying shapes results in different cloud particle volumes and therefore, in different optical thicknesses. We have modified the text as such:*

"In relation to the highest values of reflectivity the corresponding radiative forcing for Solid Columns and Droxtals are strongest with -0.20 and -0.18 W m^{-2} nm^{-1} (at 550 nm) and for Plates (10 Elements) and the mixture according to Baum et al. (2005) lowest with -0.05 and -0.06 W m^{-2} nm^{-1} (550 nm), respectively. It results in a pronounced cooling effect for Droxtals and Solid Columns, according to the highest values of optical thickness, while the effective radius is constant (see Table 1). This leads to a difference in the radiative forcing of a factor of up to 4 assuming different shapes."

Reviewer #3: Line 314: "A similar spectral trend of the shape effect shows the transmissivity" Not sure what is meant here.
Reply:
The "similar spectral trend of the shape effect" describes the likely spectral dependence in the absorptivity and transmissivity, assuming different ice crystal shapes.
Sorry for the misunderstanding, now the sentence is rearranged.

"A similar behavior can be seen in the spectral trend of the transmissivity."

Reviewer #3: Line 315-325: Again, are these purely shape differences?
Reply: *Thank you for bringing this up. Assuming a constant ice water content for varying shapes results in a shift of the number size distribution and therefore, in different optical thicknesses and effective radii.*

"Assuming a constant IWC of 0.395 g m^{-3} (approach II) for varying ice crystal shapes means keeping the total volume of the cirrus cloud particles constant. It causes a shift in the number size distribution and a changing R_{eff}. The reference value for the IWC is derived by assuming spherical cloud particles.
This leads to the largest variabilities between Droxtals, approximating spheres, and crystal shapes with a large surface area, such as aggregates of shapes or rosettes. For transmissivity (0.16 – 0.40) and absorptivity (0.38 – 0.44) the resulting differences are no more than 60 %. The largest differences are obtained for the reflectivity (0.10 – 0.40, factor of 4) as well as for radiative forcing (-0.25 – -0.52 W m^{-2} nm^{-1}) by a factor of 2, due to the link between the total surface area of a cloud and its capability of reflection. This can be seen in the inverse relation between τ and r_{eff} in Table 1, as well.
In comparison with approach I the second scenario II shows significantly larger variabilities assuming different shapes for the cloud optical layer properties and radiative forcing."

Reviewer #3: Line 355: "It is noticeable that there is a sign changing effect on RF' with negative values for the visible spectral range and a positive radiative forcing in the near infrared range" I think the author is discussing Figure 12(e). Is there really positive forcing in the near-infrared? Hard to see in this plot.
Reply: *Sorry for the small illustration of the radiative forcing curve. In the wavelength range of 1950 nm to 2100 nm a slight positive radiative forcing is observed with a maximum value of 0.002 W m^{-2} nm^{-1}.*

Reviewer #3: Line 358: Absolute values here please.
Reply: *Thank you for this helpful advice. Now, absolute values are added to the manuscript where percentage differences are given.*

Reviewer #3: Line 381-382: "It is noticeable that the cloud optical thickness of the low cloud in comparison to the cloud top height has a significant effect on the radiative forcing of the above lying cirrus". Re-word here, difficult to make sense of what is being said here. This needs to be better explained.
Reply: *Thank you for this advice, we have changed the sentence.*

"It is noticeable that the effect due to the optical thickness of the low cloud (a) in comparison to the effect of the cloud top height (b) has a stronger influence on the radiative forcing of the above lying cirrus."

Reviewer #3: Line 404: Again, references to shape differences without sizes and only relative differences (a factor of 2) quoted.
Reply: *Please, see the comment concerning line 358.*

Reviewer #3: Line 415: Differences between modeling and measurements are attributed to shape differences and mixtures of shapes. No mention of the sampling issues, or possible measurement problems.
Reply: *Thank you for making this point. As the number size distribution was derived during the measurement flight, no information about the ice crystal shape was sampled. Furthermore, the low-level cloud has a significant influence on the optical properties of the cirrus and has to be investigated, too, such as optical thickness, cloud top height, as well as vertical extent. We have modified the text accordingly.*

"The application of measured in situ microphysical properties as input of radiative transfer simulations did not accurately reproduce the measured cirrus optical layer properties. This is partly due to a variety of possible ice crystal shapes and mixtures of shapes, which was not measured, and influenced by a changing albedo during the flight. As the low level cloud has a significant influence and was not investigated during the measurement flights, more information of the water cloud is needed as well."

Manuscript prepared for Atmos. Chem. Phys.
with version 2014/09/16 7.15 Copernicus papers of the LaTeX class copernicus.cls.
Date: 23 March 2016

Spectral Optical Layer Properties of Cirrus from Collocated Airborne Measurements and Simulations

Fanny Finger[1,5], Frank Werner[1,2], Marcus Klingebiel[3], André Ehrlich[1], Evelyn Jäkel[1], Matthias Voigt[3], Stephan Borrmann[3,4], Peter Spichtinger[3], and Manfred Wendisch[1]

[1]Leipzig Institute for Meteorology (LIM), University of Leipzig, Germany
[2]University of Maryland (UMBC), Physics Department, Baltimore, Maryland, USA
[3]Institute for Atmospheric Physics, Johannes Gutenberg University Mainz, Germany
[4]Max Planck Institute for Chemistry, Mainz, Germany
[5]Now at Dr. Födisch Umweltmesstechnik AG, Markranstädt, Germany

Correspondence to: F. Finger
f.finger@uni-leipzig.de

Abstract. Spectral upward and downward solar irradiances from vertically collocated measurements above and below a cirrus layer are used to derive cirrus optical layer properties such as spectral transmissivity, absorptivity, reflectivity, and cloud top albedo. The radiation measurements are supplemented by in–situ cirrus crystal size distribution measurements and radiative transfer simulations based on the microphysical data. The close collocation of the radiative and microphysical measurements, above, beneath and inside the cirrus, is accomplished by using a research aircraft (Learjet 35A) in tandem with the towed sensor platform AIRTOSS (AIRcraft TOwed Sensor Shuttle). AIRTOSS can be released from and retracted back to the research aircraft by means of a cable up to a distance of 4 km. Data were collected in two field campaigns over the North Sea and the Baltic Sea in spring and late summer 2013. Exemplary results of one measurement flight are discussed to illustrate the benefits of collocated sampling. The radiative transfer simulations were applied to quantify the impact of cloud particle properties such as crystal shape, effective radius r_{eff}, and optical thickness τ on cirrus spectral optical layer properties. Furthermore, the radiative effects of low–level, liquid water (warm) clouds as frequently observed beneath the cirrus are evaluated. They may cause changes in the radiative forcing of the cirrus by a factor of 2. If low–level clouds below the cirrus are not taken into account the radiative cooling effect (caused by reflection of solar radiation) due to the cirrus in the solar (shortwave) spectral range is significantly overestimated.

1 Introduction

Significant uncertainties in atmospheric and climate modelling originate from the insufficient description of effects and interactions of clouds with solar and terrestrial radiation (IPCC, 2013). In particular, cirrus clouds are critical; they mostly warm but can also cool the atmosphere, depending on their optical layer properties (reflectivity, transmissivity, and absorptivity Lynch et al., 2002). Cirrus clouds globally occur at various latitudes and in all seasons with a mean global coverage of about 20 – 30 %. More than 70 % of cirrus are observed in the tropics (Wylie et al., 1994), forming relatively stable and long–lived cloud layers (Liou, 1986). Due to different meteorological conditions and evolution processes, cirrus layers are characterized by a wide diversity of macrophysical appearances, different sizes and numbers of ice particles, crystal shapes and orientations. Common horizontal and vertical inhomogeneities of these properties increase the complexity of cirrus. The optical layer properties of cirrus depend mainly on their microphysical (effective radius r_{eff}, ice water content IWC), ice crystal characteristics.

Cirrus inhomogeneities and varying crystal shapes impact (i) the energy budget of the Earth's atmosphere, and (ii) the remote sensing of cirrus optical thickness τ and r_{eff}. The simulations involved in both fields (energy budget and remote sensing) are usually based on one–dimensional (1D) radiative transfer modelling, although significant three–dimensional (3D) effects on solar radiation have been reported. For example, Schlimme et al. (2005) found that the horizontal variability of the extinction coefficient leads to significant differences in the solar irradiance fields below and above the cloud as simulated by 1D and 3D radiative transfer models, which results in a variability of transmittance of about 80 %. Zhang et al. (1999) reported that the net (solar plus terrestrial) radiative forcing of cirrus may switch sign depending on the habits and sizes of the ice crystals of the cirrus. The impact of ice crystal shape on the cirrus radiative forcing, depending on the solar zenith angle, can vary between 10 and 26 % for the solar spectral range (Wendisch et al., 2005), while for the thermal infrared spectral range even larger relative differences of up to 70 % are found (Wendisch et al., 2007). Eichler et al. (2009) investigated the influence of ice crystal shape on the retrieval of τ and r_{eff} and reported effects of up to 70 % for τ and 20 % for r_{eff}.

Measurements of spectral optical layer properties of cirrus are rarely available. Commonly, a combination of measurements and simulations is applied to derive the optical layer properties, whereby τ and r_{eff} are retrieved from reflected radiance (airborne or spaceborne) (see Francis et al., 1998) and then used in combination with a radiative transfer model to simulate layer reflectivity, transmissivity, and absorptivity.

Airborne measurements of cirrus optical layer properties are hard to obtain if only one aircraft is used, which cannot perform simultaneous measurements of irradiance above and below the cirrus as required to derive the optical layer properties. Usually, the radiative measurements above and below the cirrus are performed consecutively (e.g., Pilewskie and Valero, 1992), or using two aircrafts, one below and the other one above the cirrus. Both methods unavoidably involve temporal shifts be-

tween the two measurements above and below the cirrus and, thus, can be applied for rather static and horizontal homogeneous cloud layers only. Therefore, helicopter–borne towed platforms have been developed and adapted, such as the Airborne Cloud Turbulence Observation System (ACTOS) for microphysical in situ instruments, and the Spectral Modular Airborne Radiation measurements sysTem – HELIcopter–borne Observations of Spectral Radiation (SMART–HELIOS) for solar spectral reflectivity measurements (Henrich et al., 2010; Werner et al., 2013, 2014). For cirrus measurements, Frey et al. (2009) introduced the aircraft–borne AIRTOSS (AIRcraft TOwed Sensor Shuttle), shown in Fig. 1, which enabled to perform collocated radiation (above) and microphysical (within, in situ) measurements above and within the cirrus, mostly to check the remote sensing of crystal microphysical properties with in situ data. However, Frey et al. (2009) did not allow for collocated radiation measurements above and below cirrus because the radiation sensors were installed on the aircraft only.

In this paper we report on a significantly improved sensor setup with radiation measurements on both the aircraft and the towed sensor platform (AIRTOSS) allowing to conduct truly collocated radiation measurements for the first time. In Section 2 the instrumentation of the aircraft and of the extended setup of AIRTOSS is described. In particular, the solar spectral radiation instruments and their unique combination to deduce cirrus optical layer properties are discussed in Section 3. In Section 4 the calculated solar spectral layer properties of cirrus and the concurrent microphysical observations are introduced for one exemplary measurement case. Based on these data radiative transfer simulations are performed and analyzed in Section 5.

2 Instrumentation

The instruments were mounted at three different positions: on the aircraft (Section 2.1), an additional wing pod underneath the left wing (Section 2.1), and the towed platform AIRTOSS (Section 2.2) as illustrated in Fig. 2 (a). The operation of the aircraft together with the tethered AIRTOSS is certified for altitudes up to 12.5 km (the previous ceiling limitation was 7.6 km; Frey et al., 2009).

2.1 Aircraft

The aircraft certified for the operation of AIRTOSS is a Learjet 35A. Instruments for measurements of trace gases and water vapor are mounted inside the cabin with special inlets sampling ambient air from outside the aircraft during the flight. The analysis of the collected trace gas data is published elsewhere (Mueller et al., 2015). An upward looking radiation sensor, measuring the downward spectral irradiance $F^{\downarrow}$ (in $\mathrm{W\,m^{-2}\,nm^{-1}}$), was mounted on the fuselage including the Spectral Modular Airborne Radiation measurement syStem (SMART) inside the aircraft, introduced by Wendisch et al. (2001), and further developed by Bierwirth et al. (2009). Optical fibers connect the optical inlet with two Zeiss spectrometers for the visible to near–infrared (300 – 2200 nm) wavelength range

with a resolution (Full Width at Half Maximum, FWHM) of 2 – 3 nm (visible) and 9 – 16 nm (near–infrared), respectively. An active horizontal stabilization platform (Wendisch et al., 2001) was operated to assure the horizontal levelling of the upward looking optical inlet on top of the aircraft during the aircraft measurements. A pod mounted under the left wing of the aircraft contains another optical inlet with a pair of spectrometers, measuring the upward spectral irradiance $F^{\uparrow}$. A Forward Scattering Spectrometer Probe (FSSP–100), placed at the tip of the wing pod, measures the cloud particle number size distribution (size diameter range from 2 to 47 µm, Gayet et al., 2002). To correct for shattering (Korolev et al., 2013) the FSSP–100 records the individual data particle–by–particle (Field et al., 2003, 2006). The instrument clearly indicated the time periods when the aircraft was inside clouds.

2.2 AIRTOSS

AIRTOSS, as shown in Fig. 2 (b), has a length of 2.85 m and a diameter of 24 cm; the maximum payload is 40 kg. AIRTOSS can be released from and retracted to the aircraft by a 4 km long towing cable.

In the front part of AIRTOSS in flight direction the Cloud Combination Probe (CCP, see e.g., Wendisch and Brenguier, 2013; Klingebiel et al., 2015) is installed. The CCP consists of the Cloud Droplet Probe (CDP) and the Cloud Imaging Probe instrument (CIP grey scale – denoted as CIPgs in the following). The CDP measurement principle is similar to the FSSP–100; it detects particles in the size diameter range between 2 µm and 50 µm by measuring the forward–scattered light of a laser beam which hits the ice crystals in the cirrus. The CIPgs records two–dimensional (2D) shadow images of the cirrus particles and covers a size range between 15 µm and 960 µm with an optical resolution of 15 µm. The performance of these microphysical cloud probes in cirrus clouds was characterized by McFarquhar et al. (2007).

The center part of AIRTOSS contains a battery for power supply, which is sufficient to assure electrical power for measurements of about two hours. The radiation setup is mounted in the backward part of AIRTOSS. It consists of two spectrometer pairs and two optical inlets, one upward– and one downward–looking, measuring the downward and upward spectral irradiances $F^{\downarrow}$ and $F^{\uparrow}$. Additional sensors for static air temperature and relative humidity, latitude, longitude and position angles pitch, roll and heading of AIRTOSS are installed.

The housing of the towed platform consists of an aerodynamic canister to avoid irregular movements and to enable stable flights, which is crucial for reliable radiation measurements (Frey et al., 2009).

3 Cirrus optical layer properties

Four optical inlets, two for upward and two for downward irradiance measurements were mounted on the Learjet 35A and AIRTOSS. This setup enabled simultaneous measurements of the irradiance

in two different altitudes (e.g., above and below cloud) as required for the derivation of cirrus optical layer properties (see Fig. 3). By measuring the upward and downward irradiances at the top and base of a cloud layer the optical properties are derived by the following equations. The reflectivity R is given by:

$$R = \frac{F^{\uparrow}{}_{\text{top}} - F^{\uparrow}{}_{\text{base}}}{F^{\downarrow}{}_{\text{top}}}. \tag{1}$$

R quantifies the relative portion of incoming solar radiation that is reflected by the cloud layer. The transmissivity T of a cloud layer is defined by:

$$T = \frac{F^{\downarrow}{}_{\text{base}}}{F^{\downarrow}{}_{\text{top}}}. \tag{2}$$

T describes the part of the incoming irradiance transmitted through the cloud. The relative portion of irradiance absorbed inside the cloud layer is defined by the absorptivity:

$$A = \frac{(F^{\downarrow}{}_{\text{top}} - F^{\uparrow}{}_{\text{top}}) - (F^{\downarrow}{}_{\text{base}} - F^{\uparrow}{}_{\text{base}})}{F^{\downarrow}{}_{\text{top}}}. \tag{3}$$

Equation 3 implicitly assumes that there are no horizontal components of radiative flux divergence, only vertical flux divergences are considered to derive absorptivity by Eq. 3. From these definitions it follows:

$$R + T + A = \frac{F^{\uparrow}{}_{\text{top}} - F^{\uparrow}{}_{\text{base}} + F^{\downarrow}{}_{\text{base}} + F^{\downarrow}{}_{\text{top}} - F^{\uparrow}{}_{\text{top}} - F^{\downarrow}{}_{\text{base}} + F^{\uparrow}{}_{\text{base}}}{F^{\downarrow}{}_{\text{top}}} = 1. \tag{4}$$

In addition to the three optical layer properties defined by Eqs. 1–3, the cloud top albedo R_{top} is given by:

$$R_{\text{top}} = \frac{F^{\uparrow}{}_{\text{top}}}{F^{\downarrow}{}_{\text{top}}}. \tag{5}$$

R_{top} describes the cloud reflection property of the cloud layers and the underlying surface. For investigating the effect of a cirrus layer on the atmospheric radiative energy budget the radiative forcing (RF_{toa}) at the top of atmosphere (toa) is used, which is defined by:

$$RF_{\text{toa}} = (F^{\downarrow}{}_{\text{toa}} - F^{\uparrow}{}_{\text{toa}})_{\text{cloud}} - (F^{\downarrow}{}_{\text{toa}} - F^{\uparrow}{}_{\text{toa}})_{\text{clear sky}}. \tag{6}$$

The subscripts "cloud" and "clear sky" indicate measurements or simulations in cloudy conditions and in a clear sky (i.e., an atmosphere containing no clouds) atmosphere. Following Eq. 6, RF_{toa} is the net of solar (shortwave) and terrestrial (longwave) radiation for the atmospheric conditions. A positive RF_{toa} indicates a net warming effect of the cloud by absorbing outgoing energy from the Earth's surface. A negative RF_{toa} indicates a net cooling effect mainly due to reflecting of incoming solar radiation. The following investigations are focused on the solar spectrum from 300 nm to 2300 nm.

4 Observations

Measurements were performed during two observational campaigns in spring (6 – 8 May) and late summer (29 August – 5 September) in 2013. The research flights were based at the military airports in Hohn and Jagel, North Germany, and were carried out in restricted flight areas above the North and Baltic Sea. The measurement areas represent rectangles with the size of 50 x 80 km^2, and 35 x 80 km^2, respectively. Stepwise horizontal flight patterns were flown to collect radiative and microphysical data at different altitudes (6 – 11.5 km). In total, twelve measurement flights were carried out during both campaigns.

Measurements are presented of one exemplary flight which took place west of the German island of Helgoland above the North Sea (54.98° – 54.43°N, 6.59° – 7.57°E); it was performed on 30 August 2013 (08:33 – 09:48 UTC). Northern Germany was under the influence of an occluded front with associated cirrus and the center of the low situated south of Norway (see Fig. 4).

Fig. 4 (a) shows the corresponding composite satellite image of METEOSAT–10. In the image the cirrus is indicated by white color. Low clouds are labelled by yellow color; they were widespread over a large area, including parts of the measurement area. The flight track of the Learjet 35A is shown in Fig. 4 (b).

4.1 Microphysical measurements

Fig. 5 shows the vertical profiles of (a) static air temperature (in °C), (b) relative humidity (in %) with respect to ice, measured by instruments on the aircraft, (c) number concentration (in cm^{-3}), and (d) mean diameter (in µm), measured by the CIPgs on AIRTOSS. The bars quantify the measurement errors, resulting from instrument uncertainties (a, b), counting statistics (c), and determination of the depth of field (d). Considering the measured ice particle number concentration the cirrus was identified in altitudes between 6.7 km and 8.5 km and between 9.0 km and 9.2 km, with a temperature range of $-21\,°C$ to $-39\,°C$.

Fig. 5 (c) and (d) show the particle number concentration and mean diameter as a function of altitude. Each data point represents a mean value for a 200 m height interval. The cirrus layer between 6.7 and 8.5 km is characterized by values for the ice crystal number concentration of 1.2 x 10^{-4} cm^{-3} to 2.1 x 10^{-3} cm^{-3} and for the crystal mean diameter of 146 and 178 μm, representing an optically thin and vertically well mixed cirrus. The gaps of measured number concentration and mean diameter are due to measurements outside the observed cirrus. The second cirrus layer between 9.0 and 9.2 km altitude shows increased values for the crystal number concentration of up to 7.9 x 10^{-3} cm^{-3} and lower values for the crystal mean diameter of 33.5 to 87.4 μm. This results in an increasing optical thickness of the upper cirrus layer in comparison to the underlying cirrus layer assuming a comparable vertical extent of 200 m.

4.2 Radiation data

4.2.1 Spectral irradiances

In Fig. 6 (a) the time series of downward and upward irradiance measured by the spectrometers on AIRTOSS at an exemplarily wavelength of 550 nm is illustrated for the entire flight: gray for downward and light blue for upward irradiance. The altitude of the Learjet (dashed red line in Fig. 6 (b)) and AIRTOSS (solid red line) show the stepwise climbing flight pattern and the different altitudes of the level legs as well as the vertical distance of about 200 m between both. The gray colored peaks in the time series of the irradiance (Fig. 6 (a)) are due to flight manoeuvers and should be excluded from further analysis. The measured pitch and roll angles of the AIRTOSS were used to sort out the data with almost horizontal orientation, which is crucial for irradiance measurements (Wendisch et al., 2001). Here a threshold of 5° was assumed to accept the data. As a result the thickened line periods mark the measuring points with suitable flight legs during which the levelling of the irradiance sensors was assured. Almost constant values of the downward irradiance (1.09 – 1.20 $\mathrm{W\,m^{-2}\,nm^{-1}}$) are recorded within these time periods. The upward irradiance is influenced by the surface albedo and changing conditions due to underlying clouds; they show values between 0.56 and 0.81 $\mathrm{W\,m^{-2}\,nm^{-1}}$ at the wavelength of 550 nm.

As the AIRTOSS is towed beneath the aircraft, a horizontal displacement between the measurements on the Learjet and on the AIRTOSS needs to be accounted for. Therefore, a temporal shift of the radiation measurements on the towed platform and that measured on the Learjet 35A has to be considered to guarantee clear vertical collocation of the measurements. The temporal shift between the aircraft and AIRTOSS was calculated by using the cable length (914 m), aircraft velocity (150 – 170 $\mathrm{m\,s^{-1}}$) and altitude difference of both platforms, as a function of the true air speed. The resulting altitude and time difference varies between 160 m and 210 m, corresponding to 4.8 seconds to 6 seconds time shift.

Mean values of measured spectra of upward and downward irradiance from both platforms are shown in Fig. 7 from the time interval, indicated by the dashed lines in Fig. 6. The investigated cirrus layer is located between 9 and 9.2 km altitude and can be seen in Fig.5 (c) and (d), indicated by the upper gray colored layer. This measurement example was chosen due to the higher optical thickness, as reported in Section 4.1, and because of the low vertical extent, which enables to measure above and below this cirrus layer. Additionally, a second cirrus layer is located between 6.7 km and 8.5 km altitude and a low–level water cloud between about 1 km and 1.25 km altitude.

The vertical difference between the two measurement platforms is 195 m in the specific example discussed here. The downward irradiance $F^{\downarrow}_{\mathrm{top}}$ at the top of the cloud layer was simulated using libRadtran (Mayer and Kylling, 2005). The black solid lines in Fig. 7 show the irradiance, measured in the flight altitude of the Learjet above the cloud layer (subscript top), the black dotted lines represent the irradiance measured from the AIRTOSS at the base of the investigated part of the cirrus

layer (subscript base).

As expected, the downward irradiance below the cirrus ($F^{\downarrow}_{\text{base}}$) is lower than that measured above the cloud ($F^{\downarrow}_{\text{top}}$). This shows that the attenuation of the solar radiation (reflection and absorption by cirrus particles) by the observed cirrus can actually be quantified by observational means. The upward irradiances ($F^{\uparrow}_{\text{top}}$ and $F^{\uparrow}_{\text{base}}$) are relatively high. This is due to low clouds, which were present below the cirrus in the measurement area during the selected measurement period. In case of an atmosphere without clouds in between the cirrus and the ocean surface (dashed line in Fig. 3), lower upward irradiance data have been measured. Due to the high flight altitude, about 9.2 km, little water vapor absorption can be observed in the near infrared absorption bands as indicated by the almost unaffected downward irradiance in both levels. Therefore, most of the absorption of solar radiation, measured in the downward irradiance below the cirrus, originates from the cirrus particles itself.

The upward radiation depends on the albedo of the Earth's surface and underlying clouds, as can be seen in enhanced values of upward irradiance. The absorption bands of liquid water, as well as water vapor absorption, at wavelengths of 1140 nm or 1400 nm are obvious in the spectra. Furthermore, the irradiances $F^{\uparrow}$ at both altitudes are almost similar. In comparison to the bright surface the difference due to the cirrus is not significant.

4.2.2 Spectra of reflectivity, absorptivity, transmissivity

By measuring the spectral and collocated upward and downward irradiances at two altitudes the cloud optical layer properties of the cirrus layer are derived according to Eq. (1) – (3).

Fig. 7 (b) shows the spectral transmissivity (red, see Eq. 2), reflectivity (black, see Eq. 1), absorptivity (green, see Eq. 3), and cloud top albedo (gray, see Eq. 5) in the visible and near infrared wavelength range according to the example in Fig. 7 (a). The error bars result from the Gaussian error propagation due to uncertainties of calibration, of deviations from the ideal cosine angular sensor response correction, dark current, and signal to noise ratio. The resulting percentage errors range between 5 % and 6 % with higher values for the near infrared wavelength range.

As cirrus clouds are optically thin, the transmissivity dominates over the entire spectral range with high values between 0.88 and nearly 1. The reflectivity in Fig. 7 (b) shows very low values of not more than 0.03. This is due to the optically and vertically thin cirrus layer and a brighter water cloud underneath. The effect of the low cloud is indicated by the cloud top albedo showing high values of about 0.4 to 0.6 in the depicted wavelength range.

The transmissivity shows a slightly negative spectral slope, absorptivity a positive trend, and the reflectivity shows no spectral trend. As the imaginary part of the refractive index is associated with the absorption coefficient, which increases with increasing wavelength, the measured absorptivity shows a spectral trend with a positive slope and values up to 0.12 in the near infrared range. It points out the importance of cirrus clouds in this wavelength range.

A time series of the cloud optical layer properties (at 1640 nm) is given in Fig. 8, with (a) transmissivity, (b) absorptivity, and (c) reflectivity, for the cirrus layer between 9.0 and 9.2 km altitude and a horizontal distance of 10.4 km. The cloud top albedo from below the aircraft (gray triangles), representing the cirrus and low–level cloud, is plotted in (d).

The right panels (e)–(h) show the histograms for the respective cirrus properties in the left representing the variability during this flight part. As T, A, and R are cloud layer properties, the varying values are due to changing optical and microphysical properties of the cirrus. The layer properties of this thin cirrus show small variations, thus indicating small spatial heterogeneity of the cirrus optical layer properties. The transmissivity reveals the smallest variation between 0.890 and 0.925 (4 %). Absorptivity and reflectivity range between 0.078 and 0.098, and 0.001 – 0.008, resulting in a percentage difference of 21 % and 87 %, respectively. This is still within the error bars as shown in the left panels (b) and (c) of Fig. 8.

The larger variability of R_{top} is explained by the changing reflectivity properties of the surface on the cloud top albedo. As the cirrus layer is optically thin, R_{top} from above the cirrus is strongly affected by the surface albedo and bright underlying water clouds. This results in significant R_{top} variations between 0.35 and 0.39 representing a difference of about 11 %.

5 Sensitivity studies based on radiative transfer simulations

In this section sensitivity studies of the cirrus optical properties using radiative transfer simulations are presented. In the following the one–dimensional radiative transfer model is introduced. It is applied for individual cirrus layers as well as for atmospheric cases including a cirrus and an underlying low–level cloud.

5.1 Model introduction

To compare the measurements with simulations and for a measurement – based quantification of the impact of different parameters, such as cloud particle shape and size on cirrus cloud optical layer properties, sensitivity studies with the one–dimensional (1D) radiative transfer model libRadtran (Mayer and Kylling, 2005) are performed. Included is the DISORT (DIScrete ORdinate Radiative Transfer) code by Stamnes et al. (2000). The observed cirrus layer is represented by varying cloud properties. The corresponding upward and downward irradiances at the top and the base of the cirrus are calculated to obtain the optical layer properties reflectivity, absorptivity, and transmissivity (according to Eq. (1) – (3)), and the cloud top albedo and radiative forcing (Eq. (5) and (6)).

The required volumetric extinction coefficient $\langle b_{\text{ext},\lambda} \rangle$, single–scattering albedo $\langle \omega_\lambda \rangle$, and phase function $\langle p_\lambda \rangle$ are derived by combining calculated tables of single scattering properties by Yang et al. (2005) with a specific in situ measured number size distribution $\mathrm{d}N / \mathrm{d}D$ (in cm^{-3}) from the CCP installed on AIRTOSS. The single scattering properties for individual particles (extinction co-

efficient $C_{\text{ext},\lambda}$, scattering coefficient $C_{\text{sca},\lambda}$, single–scattering albedo ω_λ, and phase function p_λ) with different particle radii are weighted with the number size distribution. The resulting spectral volumetric properties are used as input parameters for the radiative transfer simulations. The spectral volumetric extinction coefficient $\langle \text{b}_{\text{ext},\lambda} \rangle$ in units of km^{-1} was obtained by (see Wendisch et al., 2005):

$$\langle b_{\text{ext},\lambda} \rangle = \int C_{\text{ext},\lambda} \cdot \frac{dN}{dD} \cdot dD. \tag{7}$$

The boundaries of integration are defined by the size diameter range of the CCP. A similar algorithm was used to derive the spectral volumetric single–scattering albedo $\langle \omega_\lambda \rangle$ by calculating:

$$\langle \omega_\lambda \rangle = \frac{\int \omega_\lambda \cdot C_{\text{ext},\lambda} \cdot \frac{dN}{dD} \cdot dD}{\langle b_{\text{ext},\lambda} \rangle}. \tag{8}$$

Furthermore, the volumetric phase function $\langle p_\lambda \rangle$ is obtained by:

$$\langle p_\lambda \rangle = \frac{\int p \cdot C_{\text{sca},\lambda} \cdot \frac{dN}{dD} \cdot dD}{\int C_{\text{sca},\lambda} \cdot \frac{dN}{dD} \cdot dD}. \tag{9}$$

5.2 Individual cirrus layer

To compare, in a first step, the measured cloud optical layer properties R, T, A, and cloud top albedo R_{top} with the simulated quantities, Fig. 10 (a) – (e) shows simulations of a cirrus layer between 9.0 and 9.2 km altitude with different optical thicknesses. The input for the simulations includes a measured number size distribution, shown in Fig. 9, which was measured during the AIRTOSS campaign and represents a typical cirrus. The composition of ice crystal shapes is assumed to be constant, further assuming a mixture of particle shapes according to Baum et al. (2005).

The cirrus optical thickness varies between 0.11 and 0.55. As expected, an increasing optical thickness leads to a decreased transmissivity T and increased reflectivity R, absorptivity A, and cloud top albedo R_{top}. The spectral trend shows pronounced effects for T and A in the near infrared wavelength range excluding the ranges of the water vapor absorption bands resulting in percentage differences of 8 % (0.91 – 0.98) and a factor of 5 (0.01 – 0.05), respectively, between the optically thinnest and thickest cloud layer. The absorptivity varies in the range of the ice particle absorption and causes a difference by up to a factor of 5, whereas the cloud top albedo shows a similar difference of a factor of 5 (0.007 – 0.038) in the wavelength range of water vapor absorption. R reveals the same absolute values and resulting percentage differences in the addressed wavelength range as well as in the complete wavelength range investigated here. According to the changes in the layer properties, the radiative forcing varies most between those cases while the absolute differences are small, varying between -0.006 and -0.033 $\text{W m}^{-2}\,\text{nm}^{-1}$ (at 550 nm).

Comparing the measured (diamonds) and simulated (lines) spectral cloud optical layer properties, it can be seen, that there are obvious discrepancies due to different variable input parameters such as optical thickness, ice crystal shape, and properties of the underlying surface.

As a cirrus cloud of 200 m vertical extent is not a typical one, for further sensitivity studies a cirrus between 6.7 and 8.5 km altitude is assumed, according to the measurement case of 30 August 2013 (see Fig. 5). The implemented number size distribution (Fig. 9) and the assumption of a mixture of shapes, described by Baum et al. (2005), results in a cirrus optical thickness of 1, representing a typical cirrus cloud, see Sassen and Comstock (2001) ($\tau_{\mathrm{Ci}} = 0.03 - 1.66$) and Platt et al. (1980) ($\tau_{\mathrm{Ci}} = 0.5 - 3.5$).

To investigate the effect of different ice crystal shapes (see Fig. 11), a fixed number size distribution is combined with different shape assumptions: Solid Column, Column – 8 Elements, Plate, Plate – 10 Elements, Solid Bullet Rosette, Droxtal, and a mixture of 30 % Plates (10 Elements), 30 % Hollow Bullet Rosettes, 20 % Plates, and 20 % Hollow Columns, similar to the mixture according to Baum et al. (2005). The multi–component ice crystals, such as Column – 8 Elements, are aggregates consisting of their respective number of crystals. The different crystal shapes are introduced by Yang et al. (2013). The ice crystal roughness is set to smooth, see Baum et al. (2010).

Two approaches are investigated: (I) the number size distribution is constant (NSD, left panels), (II) the ice water content is constant (IWC, right panels). While the number size distribution is derived from in situ measurements, assuming a constant IWC for a cirrus layer under constant atmospheric conditions is a more physical approach.

Fig. 11 shows the simulated (lines) spectral optical layer properties transmissivity T (a,e), reflectivity R (b,f), and absorptivity A (c,g) for those crystal shapes. Additionally, the simulated radiative forcing RF_{toa} (see Eq. 6) in (e,h) are represented. As reference case the shape Droxtal (red line) is used approximating spherical particles. Table 1 shows the resulting optical thicknesses and effective radii assuming different shapes for the two approaches.

The results for approach I show, that varying ice crystal shape causes differences that are spectrally dependent, especially for absorptivity in the near infrared wavelength range between 1450 and 1800 nm, and 1900 and 2200 nm, where the imaginary part of the refractive index of ice reveals a maximum. This corresponds to an increased absorption coefficient and, therefore, a pronounced shape effect in this wavelength range. A similar behavior can be seen in the spectral trend of the transmissivity.

The percentage difference of transmissivity between the varying shapes and the reference case (Droxtals, 0.57 at 2000 nm) ranges between 2 % and 48 %. The lowest differences show Solid Columns (0.56) and Plates, whereas the mixture according to Baum et al. (2005) and Plates (10 Elements) show highest values (0.84). The shape variability is more pronounced for reflectivity and absorptivity with differences of up to 80 % (0.078 – 0.023) and a factor of 2 (0.04 – 0.29) for Plates (10 Elements), respectively.

In relation to the highest values of reflectivity the corresponding radiative forcing for Solid Columns and Droxtals are strongest with -0.20 and -0.18 $\mathrm{W\,m^{-2}\,nm^{-1}}$ (at 550 nm), and for Plates (10 Elements) and the mixture according to Baum et al. (2005) lowest with -0.05 and -0.06 $\mathrm{W\,m^{-2}\,nm^{-1}}$

(550 nm), respectively. It results in a pronounced cooling effect for Droxtals and Solid Columns, according to the highest values of optical thickness, while the effective radius is constant (see Table 1). This leads to a difference in the radiative forcing of a factor of up to 4 assuming different shapes. Assuming a constant IWC of 0.395 g m^{-3} (approach II) for varying ice crystal shapes means keeping the total volume of the cirrus cloud particles constant. It causes a shift in the number size distribution and a changing r_{eff}. The reference value for the IWC is derived by assuming spherical cloud particles. This leads to the largest variabilities between Droxtals, approximating spheres, and crystal shapes with a large surface area, such as aggregates of shapes or Rosettes. For transmissivity (0.16 – 0.40, at 2000 nm) and absorptivity (0.38 – 0.44) the resulting differences are smaller than 60 %. The largest differences are obtained for the reflectivity (0.10 – 0.40, factor of 4) as well as for radiative forcing (-0.25 to -0.52 W m^{-2} nm^{-1}, at 550 nm) by a factor of 2, due to the link between the total surface area of a cloud and its capability of reflection. This can be seen in the inverse relation between τ and r_{eff} in Table 1, as well. In comparison with approach I the second scenario II shows significantly larger variabilities assuming different shapes for the cloud optical layer properties and radiative forcing.

5.3 Cirrus and underlying low–level cloud

Chang and Li (2005) reported an annual and global occurrence of high clouds of 52 -- 61 % (ocean – land), from which 27 % to 29 % represent cases with low clouds underneath the cirrus. During the flights very often low clouds were observed, that is why the related effect of a low–level water cloud was investigated. Fig. 12 shows two conditions, one with (black line) and one without (red line) a low–level water cloud. The cirrus is the same case as in Fig. 11, Approach I, assuming the mixture of shapes according to Baum et al. (2005). For the second case a water cloud (τ = 20) was added between 1 km and 1.25 km altitude. The measurement example is the same as shown in Fig. 7 (b). Adding a low–level cloud in the simulations leads to the strongest effects in the visible wavelength range with a higher transmissivity (0.94 to 0.99, difference of 5 %) and lower reflectivity (0.06 to 0.01, up to 85 % difference) of the cirrus layer except in the wavelength ranges of the water vapor absorption bands. The absorptivity differs rarely. A difference can be seen in the wavelength range of about 2000 nm with the largest absolute difference of 0.114 (Cirrus) to 0.134 (Cirrus + low water cloud), resulting in a percentage difference of 15 %. As the cloud top albedo is no cirrus layer property it shows the largest difference for the low–level cloud case, but a good agreement with the measurement case in the shortwave–infrared wavelength range.

For characterizing the effect of a low–level water cloud on the radiative forcing of the cirrus and the atmosphere's energy budget, a modified radiative forcing RF'_{Ci} is introduced:

$$RF'_{\text{Ci}} = RF_{\text{Ci+low cloud}} - RF_{\text{low cloud}} \qquad (10)$$

$$RF'_{\text{Ci}} = F^{\uparrow}{}_{\text{low cloud}} - F^{\uparrow}{}_{\text{Ci+low cloud}}.$$

The resulting RF'_{Ci} is the difference between the case of a cirrus with underlying low water cloud and the case with the low cloud only (as Keil and Haywood (2003) applied for aerosol layers) at the top of atmosphere.

RF'_{Ci} is shown in Fig. 12 (e) (black line) in contrast to the radiative forcing RF (see Eq. 6) of the same but single–layer cirrus (red line). This leads to an overestimation of the cooling effect of the cirrus with a percentage difference of about 80 % (-0.05 to -0.01 $\mathrm{W\,m^{-2}\,nm^{-1}}$) in the visible wavelength range and up to a factor of 2 in the near infrared range caused by the low–level cloud. Furthermore, there is a sign changing effect on RF' with negative values for the visible spectral range and a positive radiative forcing in the near infrared range (-0.002 to 0.002 $\mathrm{W\,m^{-2}\,nm^{-1}}$).

The results obtained in this paper are valid for the respective cloud cases. To evaluate the low–level cloud effect on the cirrus the properties of the low water cloud, such as optical thickness and cloud top height, have to be investigated, too. Therefore, Fig. 13 (a) and (b) show values of integrated cirrus radiative forcings (wavelength range: 300–2300 nm) with varying water cloud optical thickness (a) and cloud top height (b). The cirrus is located between 6.7 km and 8.5 km altitude and consists of the mixture of shapes according to Baum et al. (2005). The color code represents the changing cirrus optical thickness.

In Fig.13 (a) the low–level cloud is located between 1 km and 1.25 km with an increasing optical thickness from 5 to 60. In general, the cooling of the cirrus decreases with increasing optical thickness of the low–level cloud resulting in an increasing influence of the low cloud on the radiative forcing of the upper lying cirrus. An increase of radiation reflected by the lower cloud is available to interact with the cirrus compared to single cloud layer conditions. With increasing water cloud optical thickness a saturating effect becomes evident resulting in a difference of 83 % ($32\,\mathrm{W\,m^{-2}}$) for the cirrus with $\tau = 2$ and a difference of the water cloud optical thickness of 55. Additionally, with increasing cirrus optical thickness the absolute difference of RF'_{Ci} increases from $10\,\mathrm{W\,m^{-2}}$ ($\tau_{\mathrm{Ci}} = 0.5$) to $32\,\mathrm{W\,m^{-2}}$ ($\tau_{\mathrm{Ci}} = 2$).

In Fig.13 (b) the low water cloud has a constant optical thickness of 20, and a vertical thickness of 250 m with an increasing cloud top height from 1.25 to 7.25 km in steps of 1 km. Here, the amount of the reflected radiation by the low cloud, available in the cirrus level, depends on the vertical extension of the atmosphere in between and its interaction with the transmitted (from cirrus) and reflected (from water cloud) radiation. Fig.13 (b) shows a decreasing solar cooling with an increasing cloud top height of the low–level cloud. This results in a difference of $8\,\mathrm{W\,m^{-2}}$ ($\tau_{\mathrm{Ci}} = 2$) for a vertical difference of the cloud top height of 6 km. The trend of RF'_{Ci} represents a similar saturating effect with increasing cloud top height resulting in percentage differences of 20 % ($\tau_{\mathrm{Ci}} = 0.5$) to 35 % ($\tau_{\mathrm{Ci}} = 2$). It is noticeable that the effect due to the optical thickness of the low cloud (a) in comparison to the effect of the cloud top height (b) has a stronger influence on the radiative forcing of the above lying cirrus.

6 Conclusions

Solar spectra of optical layer properties of cirrus have been derived from first truly collocated airborne radiation measurements using a Learjet and the improved towed sensor platform AIRTOSS (AIrcraft TOwed Sensor Shuttle). The radiation measurements are complemented by microphysical in–situ measurements and radiative transfer simulations, based on the measured microphysical data. Two field campaigns have taken place above the North Sea and the Baltic Sea in spring and late summer 2013. The aircraft (Learjet 35A) and the towed platform AIRTOSS, released on a towing cable underneath the plane, collected radiation and microphysical data above, beneath and inside the cirrus. For radiation measurements the straight flight legs with minor changes of pitch and roll movements of the measurement platform are selected for detailed analysis.

The spectral upward and downward irradiances in the visible and near infrared wavelength range measured above and below the cirrus have been used to derive the spectral transmissivity, absorptivity, reflectivity, and cloud top albedo of the observed cirrus layer. Irradiance spectra and an exemplary time series for a straight flight leg of 30 August 2013 are analyzed. The resulting layer properties at one wavelength in the near infrared range (1640 nm) differ slightly due to horizontal inhomogeneities and the influence of low–level clouds. An increased effect due to low clouds is observed in the cloud top albedo with varying values between 0.35 to 0.39, resulting in a percentage difference of up to 11 %.

The impact of varying ice crystal shape and cloud particle size distribution is studied applying a 1D radiative transfer model in combination with volumetric extinction coefficient, single–scattering albedo, and phase function calculated from the measured ice crystal number size distributions and tables of ice crystal single–scattering properties. The results show the highest sensitivity in cloud optical layer properties for varying ice crystal shapes for the absorptivity with up to a factor of 2 with respect to the reference case of nearly spherical shaped Droxtals. The respective cirrus radiative forcing differs by a factor of up to 4 with a strong cooling effect for Droxtals. A similar effect is due to an additional low–level water cloud, as observed during the measurement flight, with a noticeable difference in the reflectivity of the cirrus of up to 85 % under multi–layer cloud conditions. The radiative forcing of the cirrus layer may switch sign and shows positive values in the near infrared wavelength range with a resulting difference of up to a factor of 2. It was found that if the low–level cloud is not considered the solar cooling of the cirrus is strongly overestimated. The variation of the low–level cloud properties cloud top height and optical thickness influences the cirrus radiative forcing, too, resulting in differences of 35 % and 83 %, respectively.

The application of measured in situ microphysical properties as input of radiative transfer simulations did not accurately reproduce the measured cirrus optical layer properties. This is partly due to a variety of possible ice crystal shapes and mixtures of shapes, which was not measured, and the impact of a changing albedo during the flight. Because the low–level water cloud has a significant influence, more information of the water cloud is needed as well. Further adjustment of the simula-

tions can probably be used to optimize the agreement and derive more information on the particle properties. The effect of the low–level water cloud has to be further investigated by varying the properties of the cirrus, such as shape, size, and height of the cloud base and top. As the interaction of the cirrus with terrestrial radiation is an important factor for affecting the Earth's energy budget, radiative transfer calculations in the terrestrial wavelength range have to be investigated in future data analysis of the field measurements.

Acknowledgements. This study was supported by the Deutsche Forschungsgemeinschaft through Project "WE 1900/19–1, BO 1829/7–1". Additional funding on a similar level for the aircraft certification of AIRTOSS and for conducting the campaign was provided by internal sources of the Particle Chemistry Department at the Max Planck Institute for Chemistry. We thank the pilots and crew of the Gesellschaft für Flugzieldarstellung (GFD) and enviscope GmbH for preparation and execution of the test and research flights, and the colleagues from Forschungszentrum Jülich and University of Warsaw for their support.

References

Baum, B. A., Yang, P., Heymsfield, A. J., Platnick, S., King, M. D., Hu, Y. X., and Bedka, S. T.: Bulk scattering properties for the remote sensing of ice clouds. Part II: Narrowband models, J. Appl. Meteor., 44, 1896–1911, 2005.

Baum, B. A., Yang, P., Hu, Y. X., and Feng, Q. A.: The impact of ice particle roughness on the scattering phase matrix RID B-7670-2011 RID B-4590-2011, J. Quant. Spectrosc. Radiat. Transfer, 111, 2534–2549, doi:10.1016/j.jqsrt.2010.07.008, 2010.

Bierwirth, E., Wendisch, M., Ehrlich, A., Heese, B., Tesche, M., Althausen, D., Schladitz, A., Müller, D., Otto, S., Trautmann, T., Dinter, T., von Hoyningen-Huene, W., and Kahn, R.: Spectral surface albedo over Morocco and its impact on the radiative forcing of Saharan dust, Tellus, 61B, 252–269, 2009.

Chang, F.–L., Li, Z.: A Near-Global Climatology of Single-Layer and Overlapped Clouds and Their Optical Properties Retrieved from Terra/MODIS Data Using a New Algorithm, J. of Climate, 18, 4752–4771, 2005.

Eichler, H., Ehrlich, A., Wendisch, M., Mioche, G., Gayet, J.-F., Wirth, M., Emde, C., and Minikin, A.: Influence of ice crystal shape on retrieval of cirrus optical thickness and effective radius: A case study, J. Geophys. Res., 114, D19203, doi:doi:10.1029/2009JD012215, 2009.

Field, P. R., Wood, R., Brown, P. R. A., Kaye, P. H., Hirst, E., Greenaway, R., and Smith, J. A.: Ice particle interarrival times measured with a fast FSSP, J. Atmos. Oceanic Technol., 20, 249–261, 2003.

Field, P. R., Heymsfield, A., and Bansemer, A.: Shattering and particle interarrival times measured by Optical Array Probes in ice clouds, J. Atmos. Oceanic Technol., 23, 1357–1370, 2006.

Francis, P., Hignett, P., and Macke, A.: The retrieval of cirrus cloud properties from aircraft multi-spectral reflectance measurements during EUCREX '93, Quart. J. Roy. Meteor. Soc., 124, 1273–1291, 1998.

Frey, W., Eichler, H., de Reus, M., Maser, R., Wendisch, M., and Borrmann, S.: A new airborne tandem platform for collocated measurements of microphysical cloud and radiation properties, Atmos. Meas. Tech., 2, 147–158, 2009.

Gayet, J. F., Auriol, F., Minikin, A., Strom, J., Seifert, M., Krejci, R., Petzold, A., Febvre, G., and Schumann, U.: Quantitative measurement of the microphysical and optical properties of cirrus clouds with four different in situ probes: Evidence of small ice crystals, Geophys. Res. Lett., 29, 83-1 – 83-4, doi:10.1029/2001GL014 342, 2002.

Henrich, F., Siebert, H., Jäkel, E., Shaw, R. A., and Wendisch, M.: Collocated measurements of boundary-layer cloud microphysical and radiative properties and comparison with satellite retrievals, J. Geophys. Res., 115, D24 214, doi:10.1029/2010JD013930, 2010.

IPCC: Climate Change 2013: The Physical Science Basis, Cambridge University Press, Cambridge, United Kingdom and New York, NY, USA, 2013.

Keil, A. and Haywood, J. M.: Solar radiative forcing by biomass burning aerosol particles during SAFARI 2000: A case study based on measured aerosol and cloud properties, J. Geophys. Res., 108, 8467, doi:10.1029/2002JD002315, 2003.

Klingebiel, M., de Lozar, A., Molleker, S., Weigel, R., Roth, A., Schmidt, L., Meyer, J., A., E., Neuber, R., M., W., and Borrman, S.: Arctic low–level boundary layer clouds: in situ measurements and simulations of mono– and bimodal supercooled droplet size distributions at the top layer liquid phase cloud, Atm. Chem. Phys., 15, 617–631, 2015.

Korolev, A. V., Emery, E. F., Strapp, J. W., Cober, S. G., and Isaac, G. A.: Quantification of the Effects of Shattering on Airborne Ice Particle Measurements, J. Atmos. Ocean Technol., 30, 2527–2553, 2013.

Liou, K.-N.: Influence of cirrus clouds on weather and climate processes: A global perspective, Mon. Wea. Rev., 114, 1167–1199, 1986.

Lynch, K., Sassen, K., Starr, D., Stephens, G., Heymsfield, A., Liou, K.-N., Minnis, P., and Platt, C.: Cirrus, Oxford University Press, New York, 2002.

Mayer, B. and Kylling, A.: Technical note: The *libRadtran* software package for radiative transfer calculations - description and examples of use, Atmos. Chem. Phys., 5, 1855–1877, 2005.

McFarquhar, G. M., Um, J., Freer, M., Baumgardner, D., Kok, G. L., and Mace, G.: Importance of small ice crystals to cirrus properties: Observations from the Tropical Warm Pool International Cloud Experiment (TWP-ICE), Geophys. Res. Lett., 34, L13803, doi:10.1029/2007GL029865, 2007.

Müller, S., Hoor, P., Berkes, F., Bozem, H., Klingebiel, M., Reutter, P., Smit, H. G. J., Wendisch, M., Spichtinger, P., and Borrman, S.: In-situ detection of stratosphere-troposphere-exchange of cirrus particles in the mid-latitudes, Geophys. Res. Let., 42, doi:10.1002/2014GL062556, 2015.

Pilewskie, P. and Valero, F. P. J.: Radiative effects of the smoke clouds from the Kuwait oil fires, J. Geophys. Res., 97, 14 541–14 544, 1992.

Platt, C. M. R., Reynolds, D. W., and Abshire, N. L.: Satellite and Lidar Observations of the Albedo, Emittance and Optical Depth of Cirrus compared to Model Calculations , Monthly Weather Review, 108, 195–204, 1980.

Schlimme, I., Macke, A., and Reichardt, J.: The impact of ice crystal shapes, size distributions, and spatial structures of cirrus clouds on solar radiative fluxes, J. Atmos. Sci., 62, 2.274–2.283, 2005.

Sassen, K., and Comstock, J. M.: A Midlatitude Cirrus Cloud Climatology from the Facility for Atmospheric Remote Sensing. Part III: Radiative Properties, J. Atmos. Sci., 58, 2.113–2.127, 2001.

Stamnes, K., Tsay, S.-C., Wiscombe, W., and Laszlo, I.: DISORT, a General-Purpose Fortran Program for Discrete-Ordinate-Method Radiative Transfer in Scattering and Emitting Layered Media: Documentation of Methodology, Tech. rep., Dept. of Physics and Engineering Physics, Stevens Institute of Technology, Hoboken, NJ 07030, 2000.

Wendisch, M. and Brenguier, J.-L.: Airborne Measurements for Environmental Research – Methods and Instruments, Wiley–VCH Verlag GmbH & Co. KGaA, Weinheim, Germany, Weinheim, Germany, iSBN: 978-3-527-40996-9, 2013.

Wendisch, M., Müller, D., Schell, D., and Heintzenberg, J.: An airborne spectral albedometer with active horizontal stabilization, J. Atmos. Oceanic Technol., 18, 1856–1866, 2001.

Wendisch, M., Pilewskie, P., Pommier, J., Howard, S., Yang, P., Heymsfield, A. J., Schmitt, C. G., Baumgardner, D., and Mayer, B.: Impact of cirrus crystal shape on solar spectral irradiance: A case study for subtropical cirrus, J. Geophys. Res., 110, D03 202, doi:10.1029/2004JD005294, 2005.

Wendisch, M., Yang, P., and Pilewskie, P.: Effects of ice crystal habit on thermal infrared radiative properties and forcing of cirrus, J. Geophys. Res., 112, D03 202, doi:10.1029/2006JD007899, 2007.

Werner, F., Siebert, H., Pilewskie, P., Schmeissner, T., Shaw, R. A., and Wendisch, M.: New airborne retrieval approach for trade wind cumulus properties under overlying cirrus, J. Geophys. Res., 118, 3634–3649, doi:10.1002/jgrd.50334, http://dx.doi.org/10.1002/jgrd.50334, 2013.

Werner, F., Ditas, F., Siebert, H., Simmel, M., Wehner, B., Pilewskie, P., Schmeissner, T., Shaw, R. A., Hartmann, S., Wex, H., Roberts, G. C., and Wendisch, M.: Twomey effect observed from collocated microphysical and remote sensing measurements over shallow cumulus, J. Geophys. Res., 119, 1534–1545, doi:10.1002/2013JD020131, http://dx.doi.org/10.1002/2013JD020131, 2014.

Wylie, D., Menzel, W., Woolf, H., and Strabala, K.: Four years of global cirrus cloud statistics using HIRS, J. Climate, 7, 1972–1986, 1994.

Yang, P., Wei, H. L., Huang, H. L., Baum, B. A., Hu, Y. X., Kattawar, G. W., Mishchenko, M. I., and Fu, Q.: Scattering and absorption property database for nonspherical ice particles in the near- through far-infrared spectral region, Appl. Opt., 44, 5512–5523, 2005.

Yang, P., Bi, L., Baum, B. A., Liou, K. N., Kattawar, G. W., Mishchenko, M. I., and Cole, B.: Spectrall consistent scatterin, absorption, and polarization properties of atmospheric ice crystals at wavelengths from 0.2 to 100 μm, J. Atmos. Sci., 70, 330–347, 2013.

Zhang, Y., Macke, A., and Albers, F.: Effect of crystal size spectrum and crystal shape on stratiform cirrus radiative forcing, Atmos. Res., 52, 59–75, 1999.

Figure 1. Photo from the Learjet 35A with towed AIRcraft TOwed Sensor Shuttle. The picture was taken during a test flight from a second aircraft. The cable was artificially thickened to make it visible in the photo.

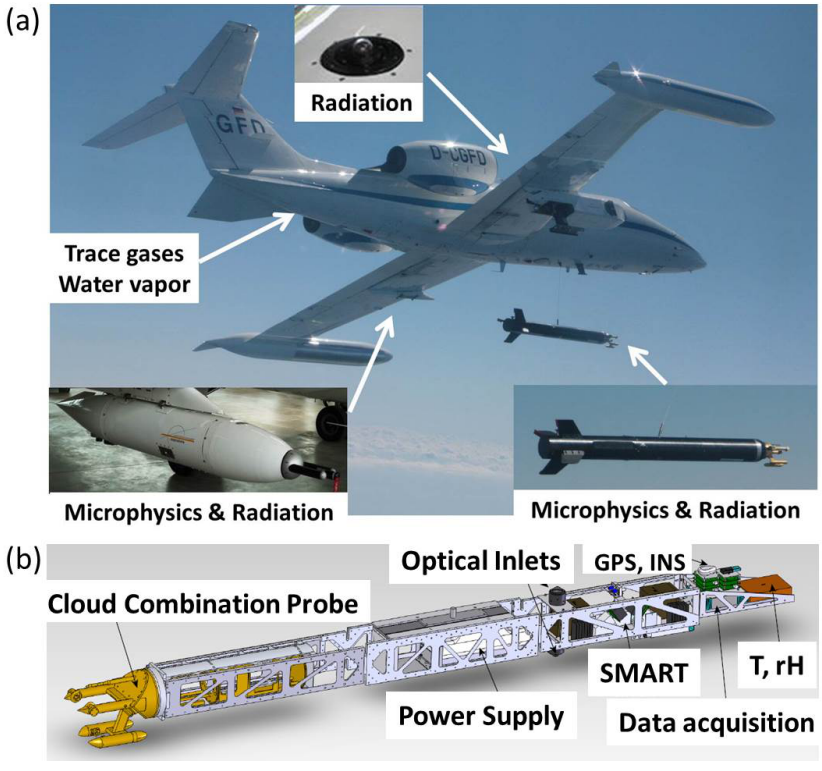

Figure 2. (a) Assembly of the research aircraft Learjet 35A, the towed AIRTOSS, and the wing pod containing instruments measuring radiation, microphysical parameter, water vapor, and trace gases. (b) Sketch of the AIRTOSS setup.

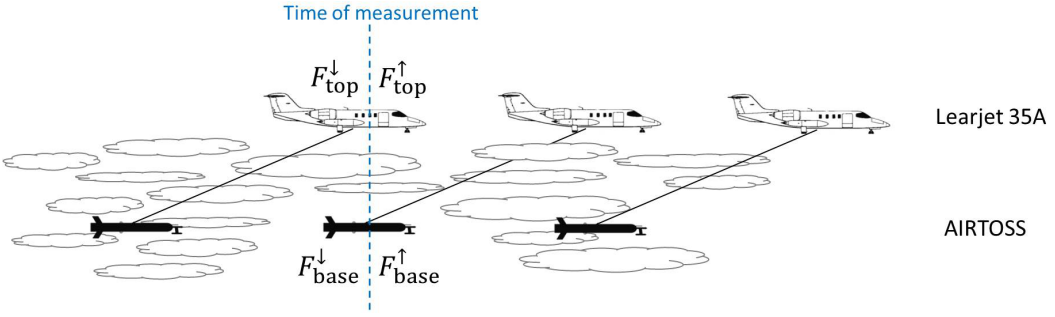

Figure 3. Schematic sketch of measurement setup to measure collocated upward ($F^{\uparrow}$) and downward ($F^{\downarrow}$) irradiance at two altitudes (base, top).

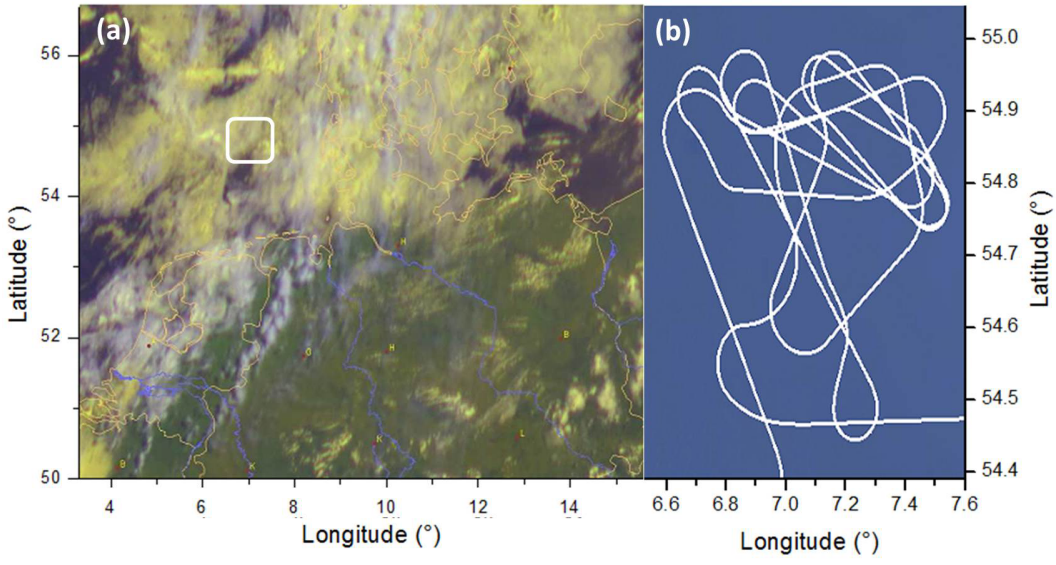

Figure 4. (a) Composite satellite image of the cloud situation on 30 August 2013 at 9:45 UTC showing cirrus (white) above yellow colored lower water clouds (Deutscher Wetterdienst / EUMETSAT). In (b) the flight track of the measuring flight in the restricted area (white box in (a)) above the North Sea near the island of Helgoland, North Germany, is shown.

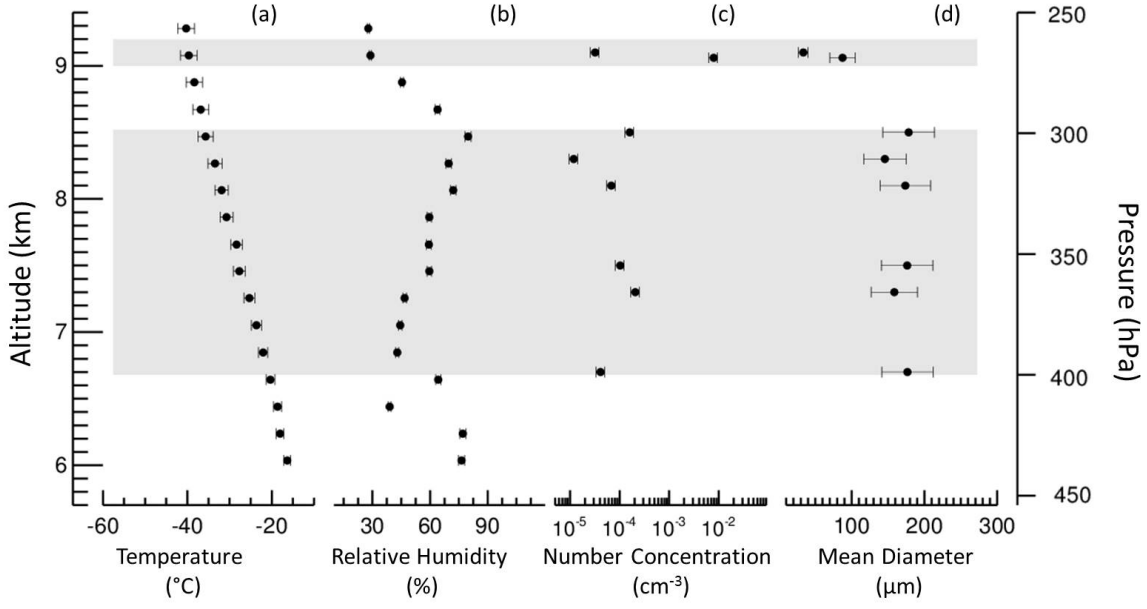

Figure 5. Vertical profiles of (a) temperature, (b) relative humidity, measured on the Learjet 35A, (c) number concentration, and (d) mean diameter, derived by CIPg on AIRTOSS, from the flight of 30 August 2013. The bars show the corresponding measurement uncertainties. The gray areas indicate the vertical extent of the cirrus layers.

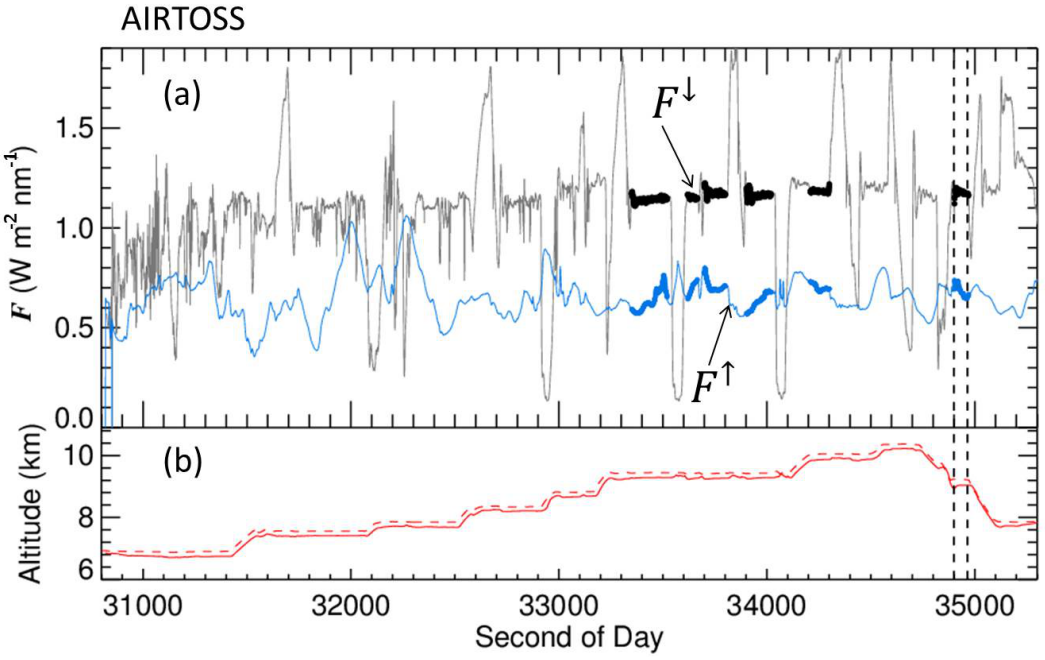

Figure 6. (a) Time series of downward (gray) and upward (light blue) irradiance F ($\mathrm{W\,m^{-2}\,nm^{-1}}$) measured on AIRTOSS at one wavelength (550 nm) from the flight of 30 August 2013. The thickened line periods mark the measuring points at straight flight legs. The red lines in (b) show the altitude of AIRTOSS (solid) and Learjet (dashed). The vertical dashed lines mark the period of the measurement example in Fig. 7.

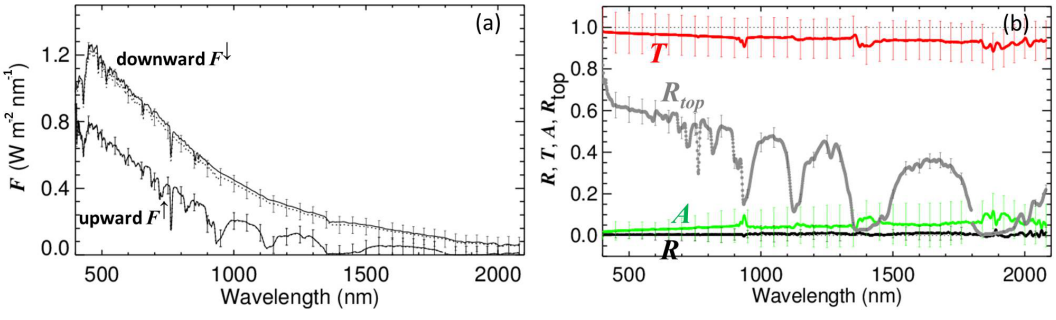

Figure 7. (a) shows measured, averaged, spectral downward and upward irradiance F from the aircraft above the cloud layer (solid lines) and AIRTOSS below the cloud layer (dotted lines) at the time period, indicated by the vertical dashed lines in Fig. 6. $F^{\downarrow}{}_{\mathrm{top}}$ is simulated. (b) shows spectral reflectivity (black), transmissivity (red), absorptivity (green), and cloud top albedo (gray) according to irradiance in (a). The vertical bars indicate the systematic errors due to measurement uncertainties.

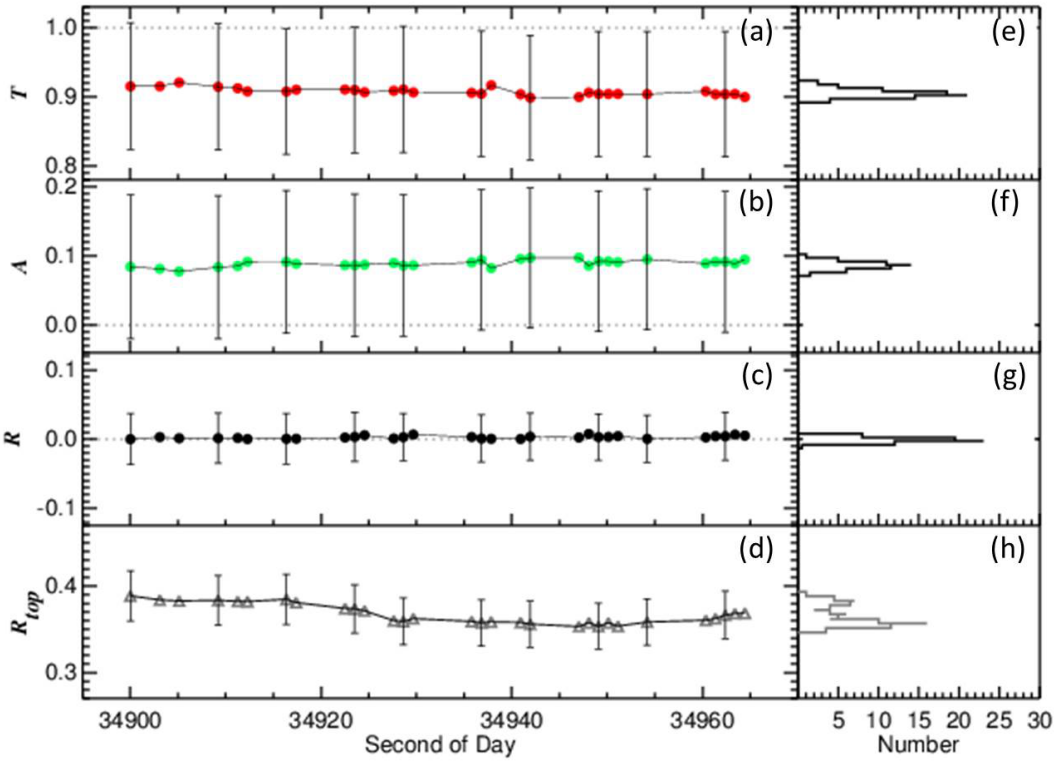

Figure 8. Shown are time series of (a) transmissivity, (b) absorptivity, and (c) reflectivity (at 1640 nm) for the cirrus layer between 9.0 and 9.2 km altitude on 30 August 2013. The associated cloud top albedo is plotted in (d). The vertical bars represent the errors due to measurement uncertainties. (e) – (h) show the histograms, respectively.

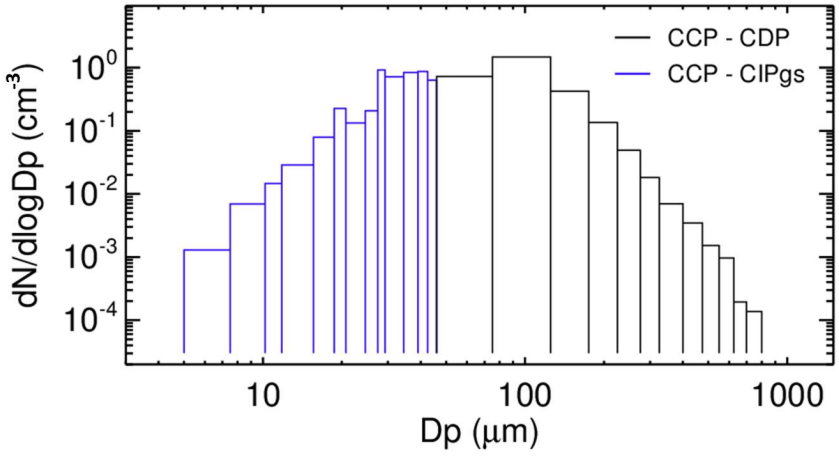

Figure 9. Number size distribution of a cirrus cloud, measured during the AIRTOSS campaign by the Cloud Combination Probe at the AIRcraft TOwed Sensor Shuttle.

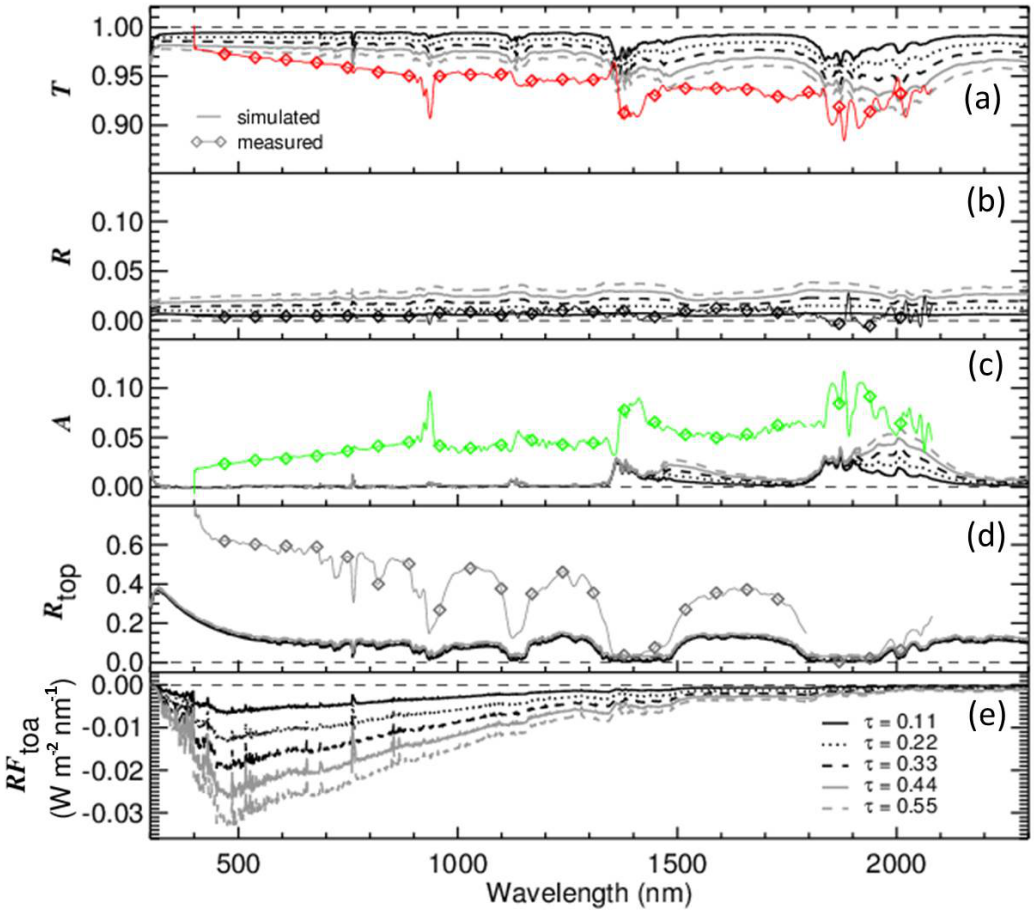

Figure 10. The lines show simulated, spectral (a) transmissivity, (b) reflectivity, and (c) absorptivity of a cirrus layer between 9 km and 9.2 km altitude. (e) are the radiative forcings at TOA, respectively. The simulations are based on a measured number size distribution assuming the mixture of shapes according Baum et al. (2005). Inserted is the measurement case (diamonds) from Fig.7.

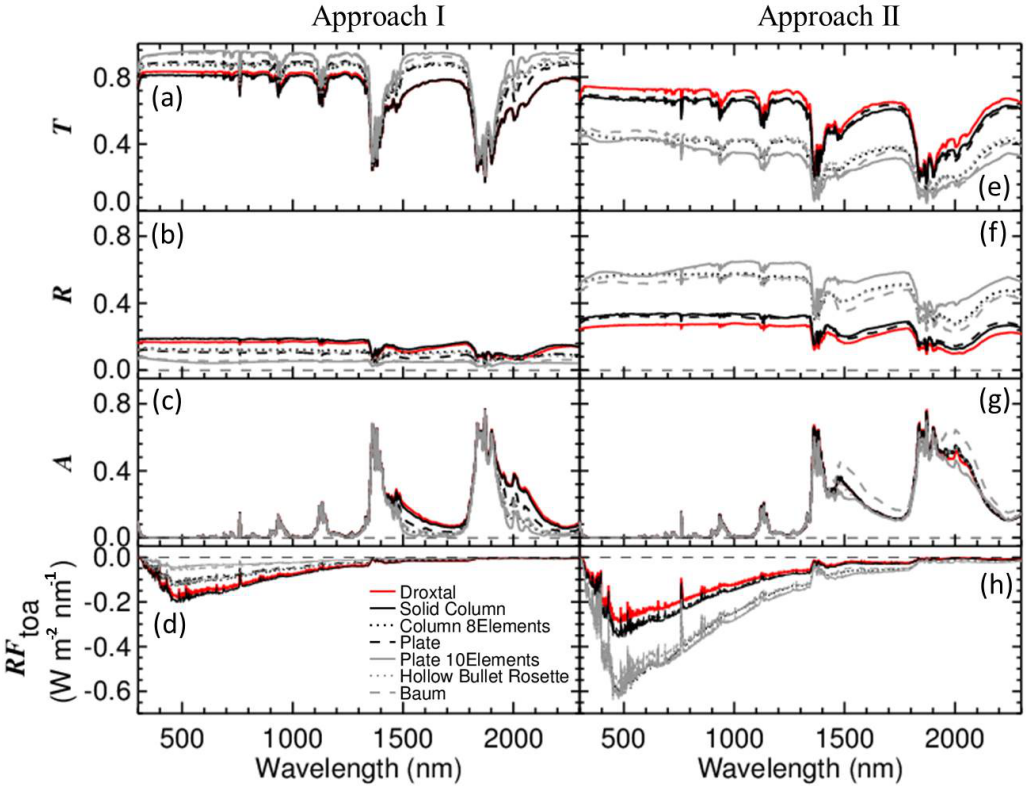

Figure 11. Shown are spectral (a,e) transmissivity, (b,f) reflectivity, and (c,g) absorptivity of a cirrus layer between 6.7 and 8.5 km altitude. (e,h) are the radiative forcings at TOA, respectively. The simulations are based on a measured number size distribution assuming different ice particle shapes. The two panels indicate two conditions: constant number size distribution (Approach I) and constant ice water content (Approach II).

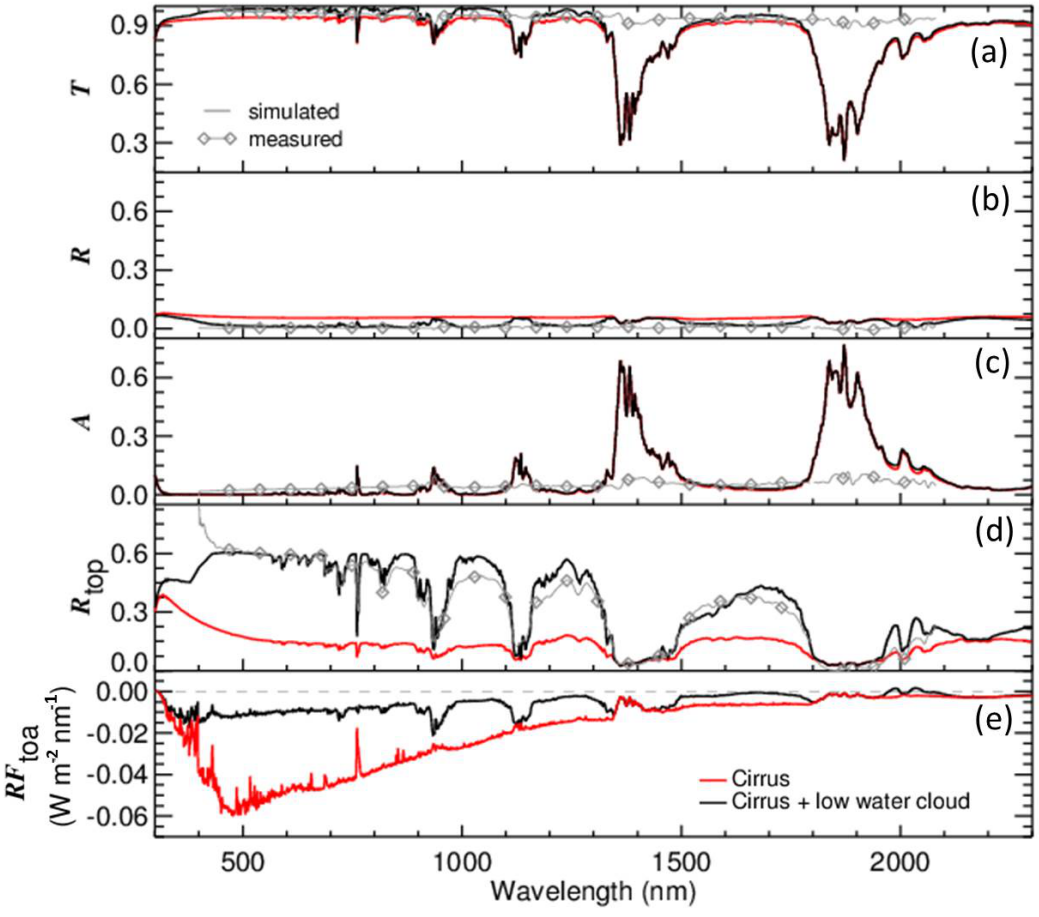

Figure 12. Same as Fig.10 assuming the mixture according to Baum et al. (2005) between 6.7 and 8.5 km altitude (τ_{Cirrus} = 1). An additional low water cloud with τ = 20 is included between 1.0 and 1.25 km altitude. Inserted is the measurement case (gray diamonds).

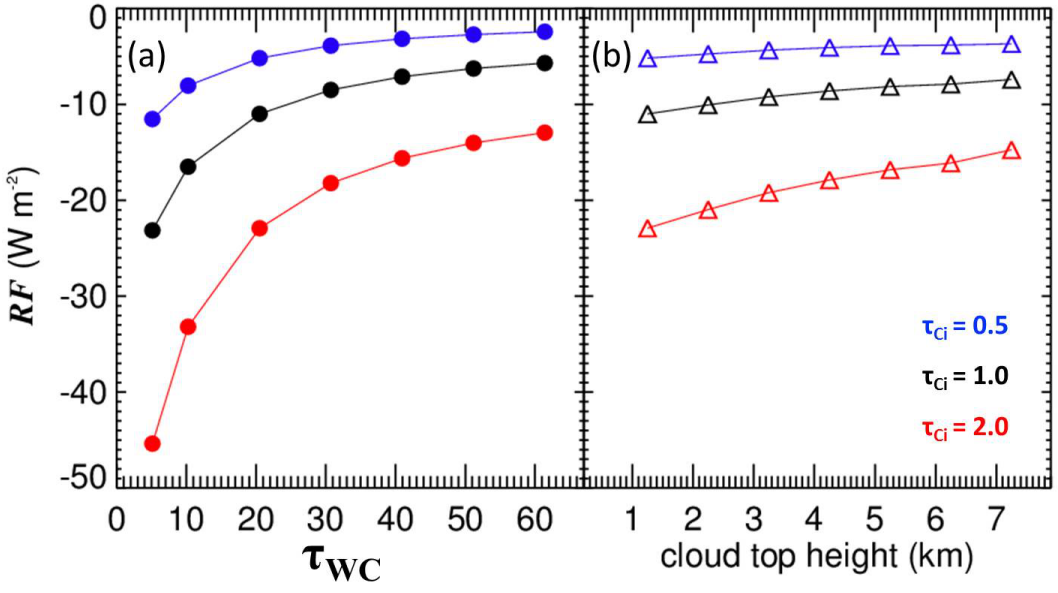

Figure 13. Integrated values of cirrus radiative forcing when a low water cloud is present. The optical thickness (left panel), and the top height (right panel) of the water cloud are varied. The colors indicate the different cirrus optical thicknesses.

Table 1. Shown are the optical thicknesses at λ=550 nm and effective radii (μ m) for a cirrus between 6.7 km and 8.5 km altitude assuming different ice crystal shapes for Approach I (constant number size distribution) and Approach II (constant ice water content).

	Approach I		Approach II	
	τ	r_{eff}	τ	r_{eff}
Droxtal	1.49	88.5	2.68	76.5
Solid Column	1.50	88.5	3.20	56.1
Column 8 Elements	0.77	88.5	7.45	27.3
Plate	1.15	88.5	4.44	28.7
Plate 10 Elements	0.54	88.5	15.4	11.9
Hollow Bullet Rosette	0.97	88.5	9.52	17.2
Baum	1.00	88.5	5.09	23.8